공학석사 학위논문

A Study on Electrochemical Decontamination of Irradiated Zr-Nb Alloys in LiCl-KCl Eutectic Molten Salts

LiCl-KCl 용융염을 이용한 방사화 지르코늄-나이오븀 합금 전해제염 연구

2016 년 **8** 월

서울대학교 대학원

에너지시스템공학부

김평화

Abstract

A Study on Electrochemical Decontamination of Irradiated Zr-Nb Alloys in LiCl-KCl Eutectic Molten Salts

Pyeonghwa Kim

Department of Energy Systems Engineering

The Graduate School

Seoul National University

The number of operational nuclear power plants over the world is 445 as of June 2016 and almost age of reactors is more than 30 years. In Korea, Kori unit #1 and Wolsung unit #1 are doing the long term operation after their design life (30years), and it is essential to replace obsolete equipment of Nuclear Power Plants (NPPs) to acquire the license renewal. For example, Wolsung unit #1 replaced Pressure Tubes (PTs). They are core components in a Pressurized Heavy Water Reactor (PHWR). Retired PTs were stored in radioactive waste storage facilities built newly in Wolsung unit #1. If the long term operation of Kori unit #1 finishes in June 2017, it will be decommissioned as related laws after sending a final decommissioning plan to an authority and receiving an approval of the decommissioning. KORAD had built the #1 underground repository cavern for low and intermediate level wastes

(LILWs) and began operating the repository in 2015. But according to KHNP's research, the LILW's repository will be saturated in 2015 due to operational wastes and decommissioning wastes. Therefore, study on decommissioning should be continued the effectively operate the repository and to reduce disposal cost for LILWs.

Zr, one of metals used in in NPPs, is so expensive metal, since a thermal neutron absorption cross section of zirconium is low and mechanical properties of zirconium are excellent, Zr based alloys are used variously in NPPs. If niobium is added to zirconium alloy, corrosion resistance of zirconium alloys is better. Zr-Nb alloys are used for structural components, claddings, pressure tubes in PWRs or PHWRs. And KAERI developed HANA claddings by adding niobium to zircaloy-4 and by modulating niobium. And have conducted verification tests in commercial reactors and research reactors. If HANA cladding is commercialized, it is expected that radioactive wastes of Zr-Nb will increase rapidly.

ORIGEN-2 computational simulation results for PHWRs pressure tubes(Zr-2.5Nb) after 30 years of operation time and 10 years of cooling time showed that specific radioactivity of Nb^{94}, Co^{60}, Fe^{55}, Ni^{63} is higher than other nuclides in the order named. In particular, Nb^{94} is critical for irradiated Zr-Nb alloys, because a half-life of Nb^{94} is 20,300 years and is longer than others. Irradiated PHWR pressure tubes by simulating ORIGEN-2 are intermediate level wastes and are need to dispose of in the cave repository as related laws. According to chapter 8.2 in the

Safety Analysis Report (SAR) of #1 LILW repository, total radioactivity of Nb^{94} is 8.59×10^{10}Bq in this repository. Based on this value, it is possible to dispose of about 10kg of irradiated pressure tubes for Nb^{94}. Considering that mass of replaced Pressure Tubes for Wolsung #1 unit is 23 ton, waste to be possible to dispose of is almost nothing. And ILWs are impossible to be disposed of in the #1 LILWs repository, because KORAD's acceptance criteria is equal to a low level waste standard, thus intermediate radioactive level of this waste should be lowered to LLWs or Very LLWs (VLLWs). If Nb^{94} is removed from irradiated pressure tubes, it will be possible to dispose of almost them. Therefore this study aims for assessment of electorefining steps to need to be exemption level wastes and decontamination effects by using electrorefining of Zr-Nb alloys.

Electrorefining of zircaloy-4 and zirlo of main materials in nuclear fuel cladding was previously studied. Their results showed that purity of zirconium at the cathode increased and concentration of impurities at the cathode decreased. Like this, it is expected to reduce Nb^{94} from radioactive wastes by using electrorefining. Molten salts used in electrorefining are mainly fluorides or chlorides. In molten salts of fluorides, a high purity zirconium is acquired and the redox behavior of Zr is one-step reaction, but operating temperature is higher than chlorides due to melting point and there is a corrosion problem. In contrast, operating temperature of chloride is low and corrosion problem occurs less than the fluoride, but disproportion reaction like that, $Zr(IV) + Zr \leftrightarrow 2Zr(II)$, occurs

because zirconium is very unstable in chloride and ZrCl is electrodeposited at the cathode. This dissertation decided to use chloride molten salts due to operating temperature.

Considering half-life and specific radioactivity of each nuclide, Nb, Co, Ni as impurities were selected to separate from PTs. After dissolving $ZrCl_4$, $NbCl_5$, $CoCl_2$, $NiCl_2$ in LiCl-KCl, cyclic voltammetry(CV) of each element is conducted at 500℃ to check the behaviors of redox for each element. Oxidation and reduction peaks were compared to previous studies and redox behaviors were checked.

CV results of Zr have usually 3 reduction peaks. For low concentration (0.2wt.%, 0.5wt.%) of $ZrCl_4$ in the molten salt, there is no reduction peak($ZrCl + e^- \rightarrow Zr$) at -1.5V(vs. Ag/AgCl). Because reduction velocity from Zr(VI) to ZrCl is slower than that from ZrCl to Zr metal. Therefore, it is expected that ZrCl is electrodeposited at a cathode in LiCl-KCl will get solved for low concentration of $ZrCl_4$. A reduction peak at -1.0V (vs. Ag/AgCl) is $Zr(IV) \leftrightarrow Zr(II)$ and a reduction peak at -1.2V (vs. Ag/AgCl) is $Zr(IV) \leftrightarrow ZrCl$. Mainly Oxidation peak was at -0.9 ~ -0.7V (vs. Ag/AgCl).

Disproportionate reaction of the niobium also occurs in LiCl-KCl, and redox behaviors of niobium are more complicated than Zr. Niobium chlorides are made up subchlorides due to nonstoichiometric reaction in LiCl-KCl. For niobium subchlorides($NbCl_y$), the value of y is from 2.33 to 3.13. A dominant subchloride is

Nb_3Cl_8. In contrast, cobalt and nickel ions are simply reduced to metals and are equal to previous studies.

Since Zr is the most oxidizing among Nb, Co, Ni as results of CV, a applied potential at a anode electrode was decided -0.85V(vs. Ag/AgCl) to dissolve only Zr. No shielding facility is in our laboratory, so irradiated material should not be used. Because Zr-2.5Nb equal to PTs material for nuclear grade couldn't be bought, HANA cladding scraps were used as surrogate materials at the anode. The lab-scale potentiostatic electrorefining experiments of unirradiated Zr-Nb alloys are conducted in LiCl-KCl-5wt% $ZrCl_4$. ICP-MS result of Zr-Nb alloys used for experiments was not included Co, Ni, so these impurities are additionally inserted to an anode basket. First, the experiment was conducted at -0.85V(vs. Ag/AgCl) as the applied potential, but there was no electrodeposition at a cathode and black powders were sunken in molten salts. Thus after oxidizing anode for 15 hours, a working electrode was changed from the anode to the cathode and the applied potential was changed to reduction potential of Zr(-1.0V~-1.6V(vs. Ag/AgCl)). At reduction potential of Zr, electrodeposition was formed at cathode and was analyzed by ICP-MS and XRD to check compositions. Results of XRD showed that the electrodeposition was mainly ZrCl, because $ZrCl_4$ concentration (5wt.%) in molten salts was higher than those of CV condition(0.1~2.0wt.%), and partailly ZrO_2 was checked at the electrodeposition. It is expected that Zr was oxidized during XRD analysis, because oxygen concentration in the glovebox was lower

than 0.1ppm. In the all of the experiment results, the purity of zirconium increased from 91~93% to 99% when anode composition before electrorefining was compare with the electrodepostion at cathde after electrorefining. A very small amount of Nb was measured, it is expect that impurities of anode for a counter electrode was chemically dissolved during electrorefining experiment and co-electrodeposit with molten salt at cathode. In all the experiment, Co was not discovered and Ni was only discovered within background concentration in LiCl-KCl. Therefore it was thought that Co and Ni would not be dissolved during electrorefining experiment.

Decontamination factors were evaluated by using results of electrorefining. And the number of electrorefining steps needed to be exemption level wastes is three. Because recovered zirconium from irradiated wastes is included Zr^{93}, one of the radioactive nuclides, it can be not recycled for general industry, but can be reused for storage drums of radioactive wastes or shielding materials in nuclear industry. Considering only one replacement of PTs for domestic four PHWRs, it is assessed that about 500 waste-drums will be reduced and economic effect is about 19 billion won.

If nuclides (Nb^{94}, Co^{60}, Ni^{63}) separated by electrorefining in molten salts or anodes are conducted nuclear transmutation to nuclides which have low radioactivity and short half-life through fast reactors or accelerators or dispose of in High Level wastes disposal repository which will be built, it is expected to solve disposal problem of radioactive wastes. Existing surface decontamination or

melting decontamination can't remove selectively activated products as this study. Therefore it is certainly necessary that volume reduction of radioactive wastes and limited recycling of valuable radioactive metals by developing electrochemical decontamination for electrorefining continuously to improve public acceptance for nuclear power as well as to reduce disposal cost and to effectively operate the repository.

Keywords: Zirconium, Niobium, Pressure Tube, Electrorefining, LiCl-KCl, Cyclic Voltammetry.

Student Number: 2014-21418

Table of Contents

List of Tables

List of Figures

1. Introduction

1.1 Background

The number of operational nuclear power plants over the world is 445 as of this year and almost age of reactors is more than 30 years like a figure 1.1 [1]. In Korea, the Kori unit #1 and the Wolsung unit #1 have operated for more than 30 years. Their life time is 30 years and after renewing their operation licenses from an authority in Korea, they are doing a long term operation. Because of aging of facilities of nuclear power plants (NPPs), NPPs replaced a few safety-related and old facilities to new one. Especially, In the Wolsung unit #1, all of the pressure tubes which play the most important role as a pressure boundary were replaced for 2 years from 2009 [2]. Total mass for Retired PTs is about 23 tons and are stored in the concrete silos of on-site dry storage facilities built newly. Low and intermediate-level wastes (LILWs) disposal repository operated by KORAD (Korea Radioactive Waste Agency) had been built in Kyung-ju from 2006 and #1 repository which has disposal capacity of 100,000 drums finished its construction in 2014 [3]. Kyung-ju LILW disposal repository will be expected to be saturated before 2055 [4]. And it is expect that radioactive waste management cost is the most highest in the decommissioning cost. Due to limitation of storage facilities and increase in LILWs disposal cost, volume reduction of radioactive wastes is a critical issue.

Alloys based on Zirconium (Zr) are used in various type of nuclear power plants since Zr has some features like followings. The thermal neutron absorption cross section of Zr is low. And it has superior mechanical properties, high hardness, high corrosion resistance, acceptable ductility. Introducing Sn, Nb, Fe, Cr, Ni into Zr improves mechanical properties like corrosion resistance [5]. In particular, Nb is main element added into Zr to improve corrosion resistance. Zr-Nb alloys are mainly used for cladding, pressure tube, structural component in the nuclear power plants which have harsh environment like high temperature, high radiation, high pressure. Zr-Nb alloys are installed near the reactor core, so they are easy to be activated products. Other Zr alloys such as Zircaloy-2, Zircaloy-4, Zirlo are mainly used for nuclear fuel claddings in Pressurized Water Reactors (PWRs). In the Republic of Korea (ROK), spent nuclear fuel of 750 metric tons are generated in every year and Zircaloy cladding makes up 25 weight percent and 40 volume percent of spent nuclear fuel [6]. Therefore, it is impossible not to generate radioactive Zr-alloys wastes during nuclear power plant operation. And Zr alloys wastes are expected to have a higher radioactive level than LLW criteria. If these wastes is reduced volume or is reused for something in the nuclear industry, it will help to operate the LILW effectively, and will reduce the decommissioning cost.

Decontamination studies for nuclear fuel claddings such as Zircaloy-4 or Zirlo have conducted in many countries to recycle Zr metal and reduce volume of radioactive wastes. But it is few study about decontamination of Zr-Nb alloys. A

typical Zr-Nb alloy is used as pressure tubes in PHWRs. And KAERI has developed HANA claddings which is made from Zircaloy-4 added niobium element to increase corrosion resistance since 1996. HANA cladding have being tested in the Halden research reactors for several years [7]. HANA cladding was verified material integrity and if it is used as a nuclear fuel cladding in all of the domestic nuclear power plants, radioactive wastes volume of Zr-Nb alloys will be expected to increase rapidly. Therefore this dissertation focuses on decontaminating Zr-Nb alloys such as pressure tubes of PHWRs.

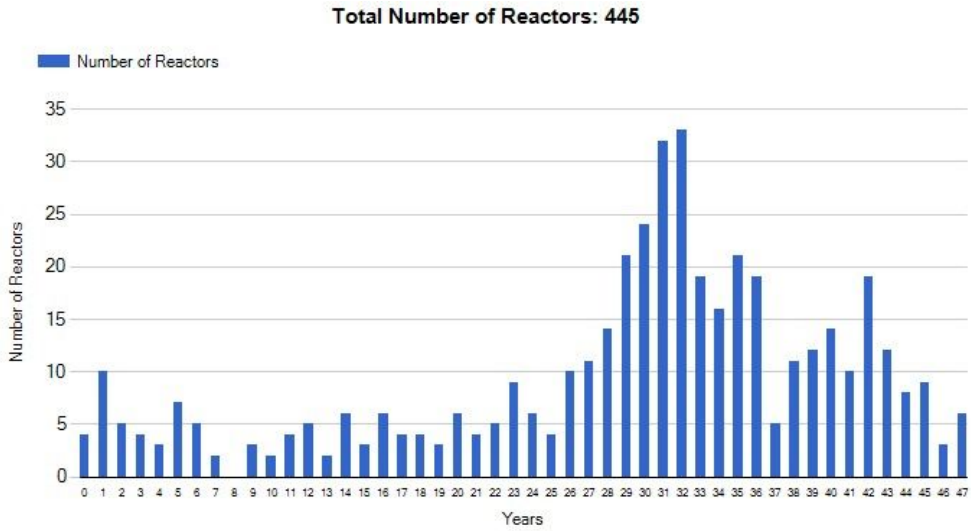

Figure 1.1 Age distribution of operating nuclear reactors worldwide (as of June 2016) [1].

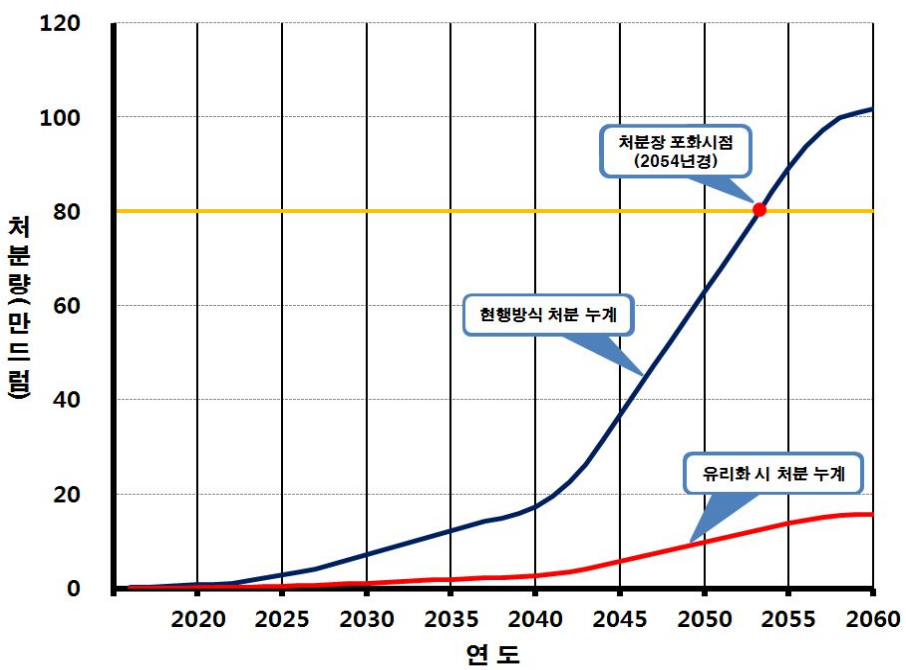

Figure 1.2 Expectation to saturation of LILWs disposal repository in KOREA [3].

Table 1.1 Zirconium-Niobium Alloys used in Nuclear Power Plants [8].

Alloy	Sn, wt.%	Nb, wt.%	Vendor (Country)	Component	Reactor Typer
ZILRO	0.7-1	1	Westinghouse	Cladding	PWR
Zr-2.5Nb	-	2.4-2.8	-	Pressure Tube	CANDU
E110	-	0.9-1.1	Russia	Cladding	VVER
E125	-	2.5	Russia	Pressure Tube	RBMK
E635	0.8-1.3	0.8-1	Russia	Structural component	VVER
M5	-	0.8-1.2	Areva	Cladding, Structural component	PWR

Table 1.2 chemical composition of HANA cladding and Zircaloy-4 cladding [7].

Alloy	Sn, wt.%	Nb, wt.%	Cu, wt.%	Component	Reactor Type
HANA3	0.4	1.5	0.1	Cladding	PWR
HANA4	0.4	1.5	-		
HANA5	0.8	0.4	0.1		
HANA6	-	1.1	0.05		
Zircaloy4	1.3	-	-		

1.2 Problem Statement

Pressure tube in PHWRs is safety-related part and one of the most important parts to operate nuclear power plant, so should be made by observing ASTM B353-12 UNS60904. As shown column 4 in figure 1.3, Pressure tube for nuclear consists of major elements such as Zr (97.5wt.%), Nb (2.5wt.%) and impurities [9].

To investigate radioactivity from activation products in irradiated pressure tubes (Zr-2.5Nb), a one-group point depletion code developed by Oak Ridge National Laboratory, ORIGEN-2, was utilized. It was assumed that fresh pressure tubes were irradiated in the maximum neutron flux ($1.0x10^{14}$ n/cm2/s) of typical PHWRs for continuous 30 years [10]. This modeling result is enough to conservative because assumptions are maximum neutron flux and continuous activation for 30 years. A number of activation products are produced during in-core neutron irradiation. As shown in figure 1.4, ORIGEN-2 computational simulation results for pressure tubes(Zr-2.5Nb) after 30 years of operation time and 10 years of cooling time showed that specific radioactivity of Co^{60}(2.37×10^{7}Bq/g), Nb^{94}(8.34×10^{6}Bq/g), Fe^{55} (4.16×10^{6}Bq/g), Ni^{63}(1.26×10^{6}Bq/g) is high in the order named. In particular, Nb^{94} is critical for irradiated Zr-Nb alloys, because half-life of Nb^{94} is 20,300 years and is longer than others. So, Nb^{94} is the most dominant nuclide for total radioactivity after 300 years from discharging pressure tubes in PWHRs. Irradiated pressure tubes by simulating ORIGEN-2 are intermediate level

wastes (ILWs) and are needed to dispose of in cave repository as related laws. According to the Safety Analysis Report (SAR) of #1 LILW repository, total radioactivity of Nb^{94} is 8.59×10^{10}Bq in this repository [11]. In reference to this value, it is possible to dispose of about 10kg of irradiated pressure tubes for Nb^{94}. By using a following relation, it can calculate mass of possible disposal wastes.

Mass of possible disposal wastes relation:

(Total radioactivity)[Bq] / (Specific Radioactivity of Waste)[Bq/g] (1)

$$\frac{8.59E+10[Bq]}{8.34E+6[Bq/g]} = 1.030E+4[g] = 10.30[\text{kg}]$$

Considering that mass of replaced pressure tubes for Wolsung #1 unit is 23 ton, it is expected not to dispose of in #1 LILWs repository. In addition, intermediate level wastes (ILWs) are impossible to be disposed of in the #1 LILWs repository, because KORAD's acceptance criteria is like a low level waste now. So these radioactive level should be changed from ILWs to LLWs or Very LLWs (VLLWs). If Nb^{94} is removed from irradiated pressure tubes, it will be possible to dispose of almost them. Additionally Ni^{63} and Co^{60} are major radioactive nuclide except Nb in considering radioactivity and half-life, Ni^{63} and Co^{60} are needed to remove from irradiated pressure tubes.

Element	Composition, Weight %				
	UNS R60001	UNS R60802	UNS R60804	UNS R60901	UNS R60904
Tin	...	1.20–1.70	1.20–1.70	...	...
Iron	...	0.07–0.20	0.18–0.24	...	...
Chromium	...	0.05–0.15	0.07–0.13	...	...
Nickel	...	0.03–0.08	...	...	...
Niobium (columbium)	...	...	...	2.40–2.80	2.50–2.80
Oxygen	*A*	*A*	*A*	0.09–0.15	*A*
Iron + chromium + nickel	...	0.18–0.38	...	...	...
Iron + chromium	...	...	0.28–0.37	...	...
	Maximum Impurities, Weight %				
Aluminum	0.0075	0.0075	0.0075	0.0075	0.0075
Boron	0.00005	0.00005	0.00005	0.00005	0.00005
Cadmium	0.00005	0.00005	0.00005	0.00005	0.00005
Calcium	...	0.0030	0.0030	...	...
Carbon	0.027	0.027	0.027	0.027	0.027
Chromium	0.020	...	...	0.020	0.020
Cobalt	0.0020	0.0020	0.0020	0.0020	0.0020
Copper	0.0050	0.0050	0.0050	0.0050	0.0050
Hafnium	0.010	0.010	0.010	0.010	0.010
Hydrogen	0.0025	0.0025	0.0025	0.0025	0.0010
Iron	0.150	...	...	0.150	0.150
Magnesium	0.0020	0.0020	0.0020	0.0020	0.0020
Manganese	0.0050	0.0050	0.0050	0.0050	0.0050
Molybdenum	0.0050	0.0050	0.0050	0.0050	0.0050
Nickel	0.0070	...	0.0070	0.0070	0.0070
Niobium	...	0.0100	0.0100	...	...
Nitrogen	0.0080	0.0080	0.0080	0.0080	0.0080
Phosphorus	...	...	...	0.0020	0.0020
Silicon	0.0120	0.0120	0.0120	0.0120	0.012
Tin	0.0050	...	...	0.010	0.010
Tungsten	0.010	0.010	0.010	0.010	0.010
Titanium	0.0050	0.0050	0.0050	0.0050	0.0050
Uranium (total)	0.00035	0.00035	0.00035	0.00035	0.00035

Figure 1.3 Chemical composition of Zr-Nb alloy used for nuclear grades (ASTM B353-12) [9].

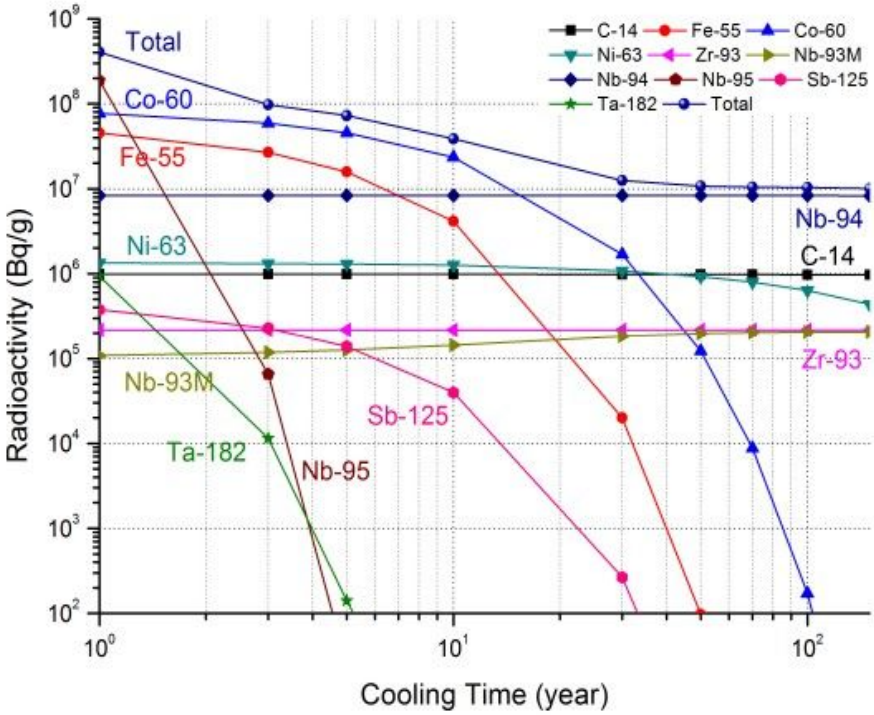

Figure 1.4 Radioactivity of CANDU pressure tubes (Zr-2.5Nb) about 30 years operation simulated by using the ORIGEN-2 code

Table 1.3 Radioactivity of CANDU pressure tubes (Zr-2.5Nb) about 30 years operation and 10 years cooling time simulated by using the ORIGEN-2 code

Element	Specific Radioactivity (Bq/g)	Half Life (years)	Emitted Radioactivity[MeV]
Nb-94	8.34×10^{6}	20,300	β^- : 0.060 γ : 0.702, 0.871
Co-60	2.37×10^{7}	5.27	β^- , γ: 2.824
Fe-55	4.16×10^{6}	2.73	E.C.*:0.231
Ni-63	1.26×10^{6}	100	β^- ,: 0.0669

[*:Electron Capture]

Table 1.4 Total Radioactivity of each nuclide in the #1 LILWs Repository [11].

Element	Total Radioactivity(Bq)
Nb-94	8.59×10^{10}
Co-60	7.22×10^{14}
Fe-55	1.68×10^{15}
Ni-63	1.85×10^{15}

2. Literature Reviews

2.1 Electrorefining studies of Zr alloys

There were several studies for electrorefining of Zr alloy to decontaminate irradiated metal wastes. There would be many methods rely on molten salt's type such as fluoride or chloride.

Chloride molten salts such as LiCl-KCl eutectic have advantages as follows, lower corrosive than fluoride molten salts and low operating temperature due to the melting point of chloride salts. C.H.Lee conducted electrorefining of zircaloy-4 in LiCl-KCl-4wt.% $ZrCl_4$ salts to separate pure Zr from zircaloy-4 [12]. Stainless steel was used as an anode basket. He experimented two electrorefining cases by controlling cathode potential. Cathode electrode was used for tungsten wire as the working electrode. Applied potentials were -1.15V (vs. Ag/AgCl) and -1.55V (vs. Ag/AgCl). The operating temperature was 500°C and experiment time was an hour. As shown figure 2.1, main XRD peaks of the depositions of cathode were ZrCl at -1.15V (vs. Ag/AgCl) and minor peaks were Zr metallic phase or ZrO, because there is disproportionate reaction of Zr in chloride molten salts such as $Zr^{4+} + Zr \rightarrow 2Zr^{2+}$. When applied potential was -1.55V (vs. Ag/AgCl), the intensity of peaks was smaller than -1.15V (vs. Ag/AgCl). And Zr purity at -1.15V (vs. Ag/AgCl) was higher than that at -1.55V (vs. Ag/AgCl). So applied potential at -1.15V (vs. Ag/AgCl) is more effective than condition at -1.55V (vs. Ag/AgCl).

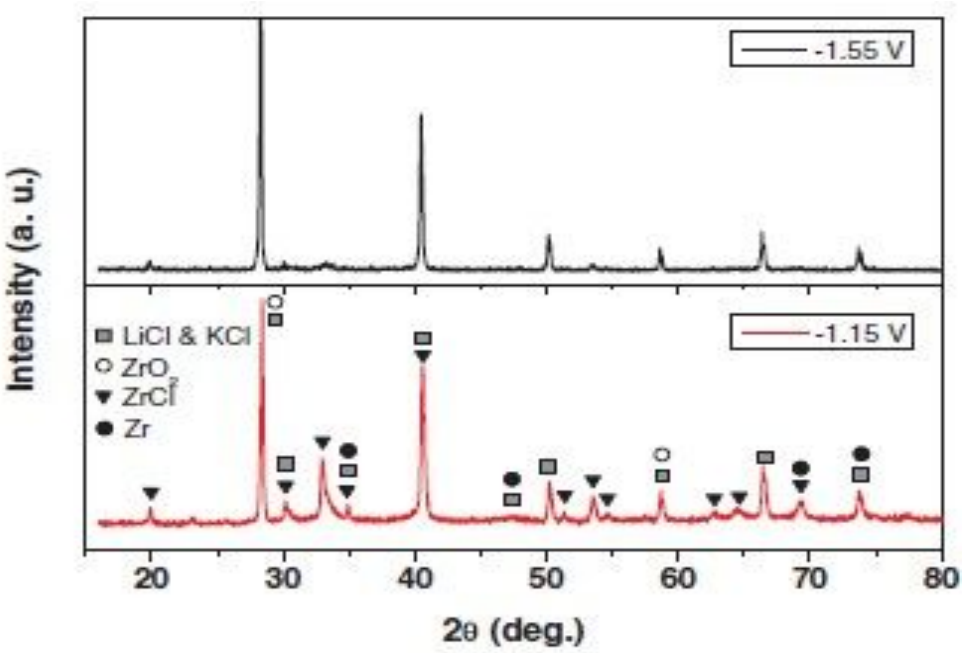

Figure 2.1 X-ray diffraction(XRD) patterns of Zr compounds deposited at -1.15 and -1.55 V (vs. Ag/AgCl) in LiCl-KCl-ZrCl4 at 500°C [12]

Figure 2.2 Zr deposits on a cathode [12].

Table 2.1 Composition analyses of recovered Zr deposits by ICP-AES [12].

Elements	Zircaloy-4 (wt.%)	Zr recovered at -1.15V (wt.%)	Zr recovered at -1.55V (wt.%)
Zr	98.23	99.44	98.95
Sn	1.45	0.56	0.87
Fe	0.14	N/D	0.14
Cr	0.1	N/D	0.04
Etc	0.08	-	-
Total	100	100	100

The electrorefining of Zirlo in LiF-KF molten salts were conducted by K.T,Park to purify Zirlo.[13] In fluoride molten salts, the operating temperature is higher than chloride molten salts due to melting point and a corrosion problem is generated, but a disproportionate reaction of Zr don't appear, so there is nearly ZrCl in a deposition of cathode. He performed cyclic voltammetry on LiF-KF-ZrF4 before electrorefining of Zirlo, and showed one-step reduction as $Zr^{4+} + 4e^{-} \rightarrow Zr$. The experimental setup is shown in figure 2.3. The operating temperature was 700°C and the working electrode was cathode. According to results of XRD for products of cathode as shown figure 2.4, major peaks are Zr and minor peaks are ZrO_2. Therefore, fluoride molten salts is more effective than chloride molten salts to acquire pure Zr. As shown in figure 2.5, denser deposits was recovered with lower applied currents [16]. And the purity of Zr in all experiments improved more, especially concentration of Nb was lower than 30ppm in figure 2.6.

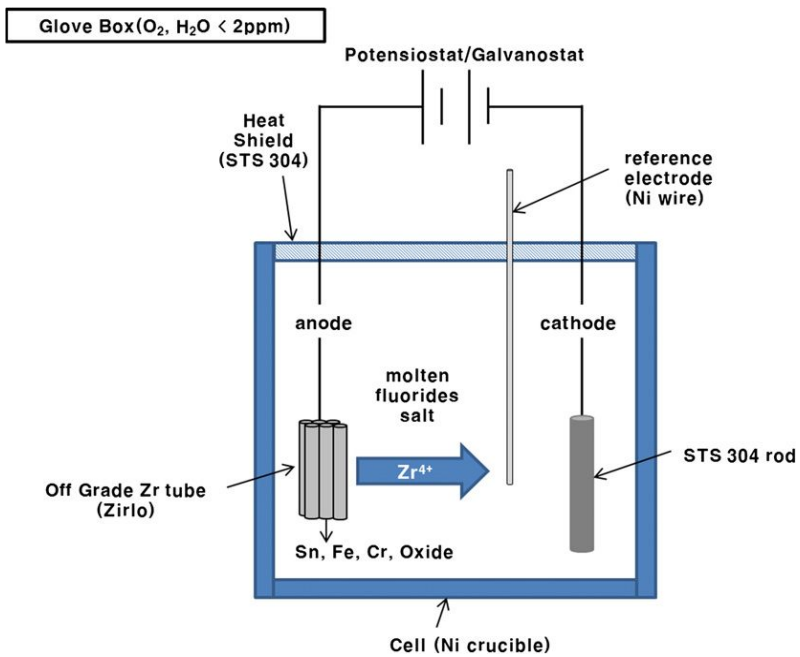

Figure 2.3 Schematic diagram of the experimental apparatus for Zr scrap electrorefining [13].

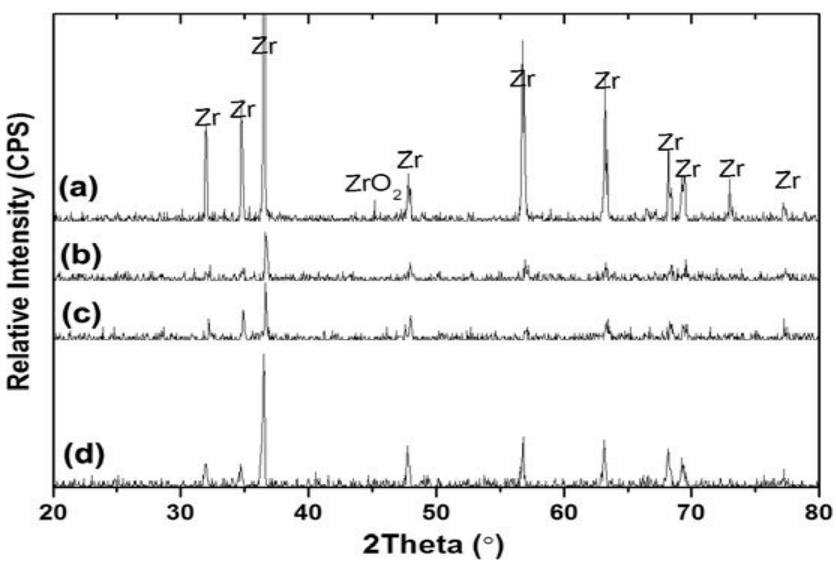

Figure 2.4 Comparisons of XRD peaks for Zr deposits under electrorefining conditions [13].

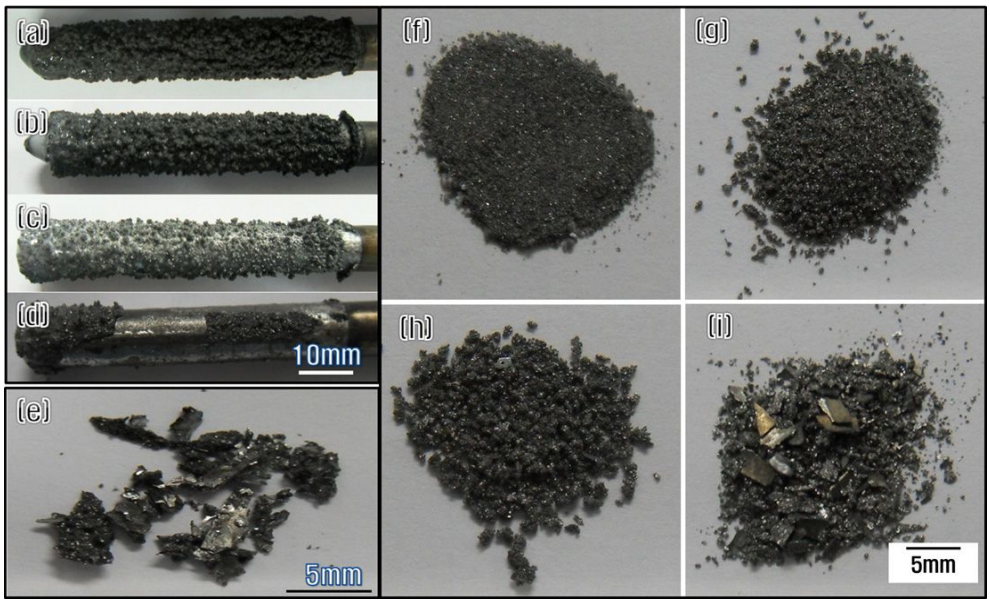

Figure 2.5 Images of cathode shapes after Zr electrorefining and images of washed Zr deposit. Cathode shapes after electrorefining [13].

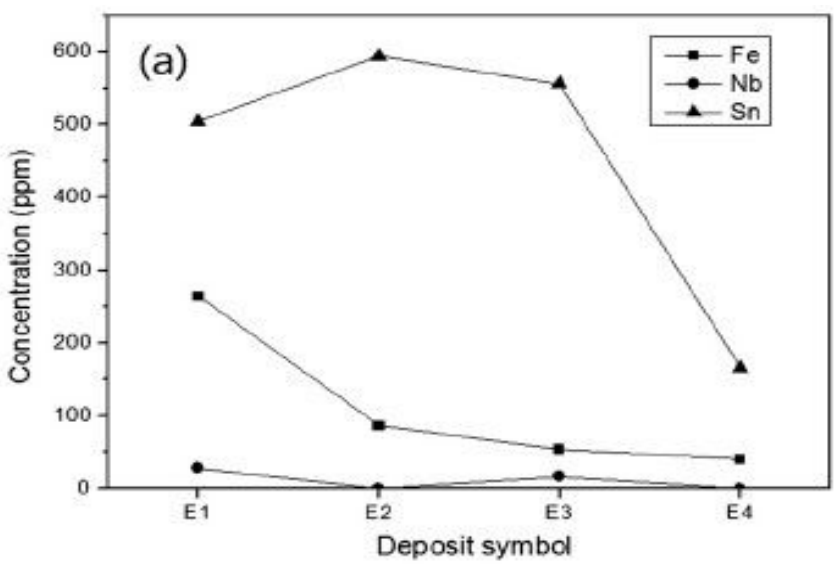

Figure 2.6 ICP results for impurities (Nb, Sn, and Fe) in Zr deposits [13].

R. Fujita conducted electrorefining of irradiated BWR channel box by using LiCl-KCl-LiF (10mol%) to make Zr(IV) stable in LiCl-KCl [15]. This study was very important that irradiated metal wastes were decontaminated by electrorefining. After first electrorefining experiments, radioactivity of Co and Sb in deposits at cathode decreased from 1E+06 Bq/g to 1E+03 Bq/g and after second experiment, radioactivity of Co and Sb was about 1E+02 Bq/g. This study revealed that the electrochemical decontamination by using electrorefining was very useful and effective.

There is the table 4.2 that shows advantages and disadvantages for each molten salt. We decided to use LiCl-KCl salts for electrorefining, because it was easy to melt salts.

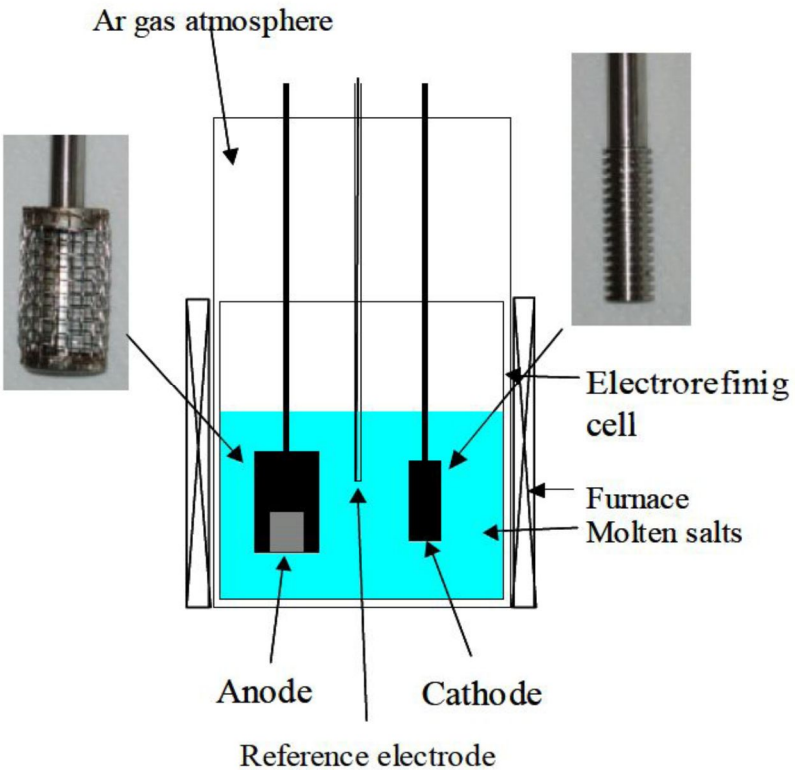

Figure 2.7 Schematic experimental apparatus used for electrorefining in LiCl-KCl-LiF [15].

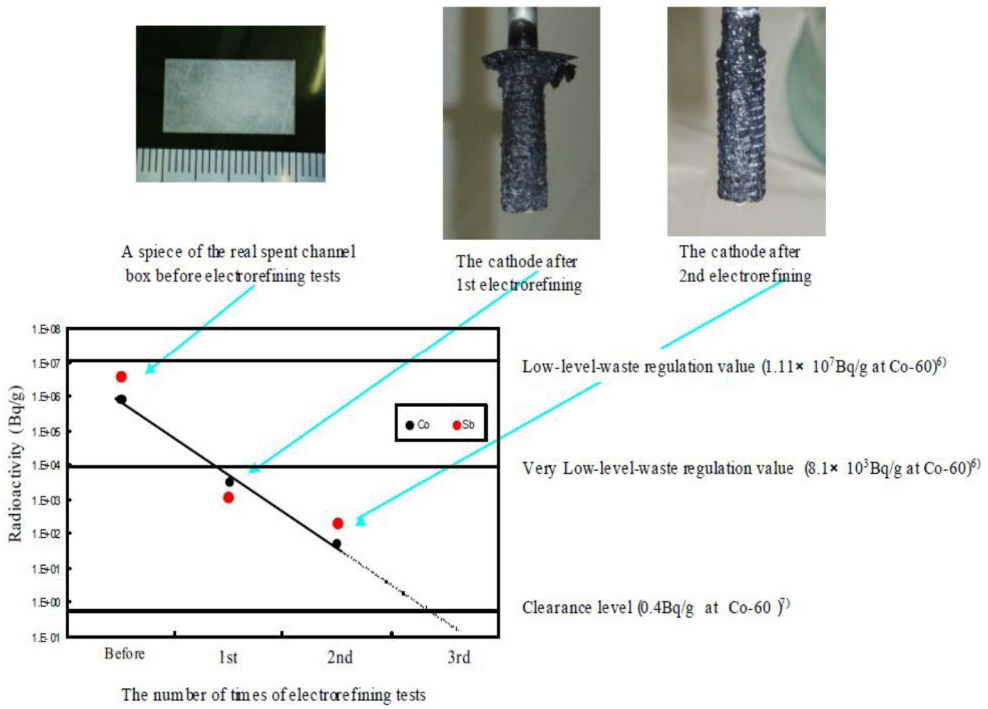

Figure 2.8 The results of two step electrorefining in LiCl-KCl-LiF [15].

Table 2.2 Comparison of Zirconium alloy decontamination process [16].

		Advantages	Disadvantages
Volume Deconta-mination	Electrorefining in fluoride salts	One-step reduction of Zr(IV) into Zr metal Metal deposition with high purity of 99.93%	High operating temperature Fluoride corrosion
	Electrorefining in fluoride-chloride salts	Suppressed disproportionate reaction Metal deposition with high purity of 99.9%	High operating temperature Fluoride corrosion Complicated salt purification
	Electrorefining in chloride salts	Low operating temperature Low corrosion problem	Disproportionate reaction ZrCl co-deposition

2.2 Electrochemistry

2.2.1 Cyclic voltammetry

There are many electrochemical methods to determine redox behaviors of elements. Of them, cyclic voltammetry (CV) is generally utilized to check a reduction potential of elements. In a cyclic voltammetry the working electrode potential is ramped linearly versus time. And the current at the working electrode is plotted versus the applied potential [17]. Reduction and oxidation reactions occur at the surface of electrode as potentials is changed. The reduction peak is negative current and oxidation peak is positive current in shown figure 2.9. CV experimental setup is commonly consisted of the three-electrode setup as reference electrode, working electrode and reference electrode. There are commonly two redox reactions, one is a reversible reaction, the other is an irreversible reaction.

Reversible reaction of redox mechanisms is generally complied with the Nernst equation and the following relation where E_{pa} is the oxidation peak potential, E_{pc} is the reduction peak, R is the universal gas constant (8.314J/mol/K), T is the absolute temperature (K), n is the number of electron in the reaction and F is the Faraday's constant (96,485 C/mol),

$$E_{pa} - E_{pc} = 2.22 \frac{RT}{nF} \quad . \tag{2.1}$$

For a reversible soluble-soluble reaction, the diffusion coefficient, D, is found

by using both peak currents of reduction and oxidation (I_{pc}, I_{pa})through the following Randles-Sevcik equation [18], where S is the working electrode surface area, C is the concentration (mol/cm^3), ν is the scan rate in voltammetry,

$$\frac{I_{pc}}{\sqrt{\nu}} = -0.4463nFSC\sqrt{\frac{nFD_{ox}}{RT}} \ , \tag{2.2}$$

$$\frac{I_{pa}}{\sqrt{\nu}} = 0.4463nFSC\sqrt{\frac{nFD_{red}}{RT}} \ . \tag{2.3}$$

The equilibrium potential can be founded by using diffusion coefficients and apparent standard reduction potential through Eq. (2.4),[19-20]

$$E = E^{0*} + \frac{RT}{nF}\sqrt{\frac{D_{red}}{D_{ox}}} \ , \tag{2.4}$$

The apparent standard reduction potential, E^{0*}, including the activity coefficients (γ) and is defined as [21]

$$E^{0*} = E^{0} + \frac{RT}{nF}\ln(\frac{\gamma_{ox}}{\gamma_{red}}) \ , \tag{2.5}$$

The equilibrium potential can be estimated by using mole fraction, X, for a soluble-insoluble reaction through the Nernst equation,

$$E^{0*} = E^{0} + \frac{RT}{nF}\ln(\frac{X_{ox}}{X_{red}}) \ , \tag{2.6}$$

For the reversible reaction in CV experiments, it is generally satisfied with

several following conditions [22]. The electron transfer rate is faster than mass transfer rate and it is easy to be found at the low scan rate. CV voltammogram is symmetry because a reduction peak current is almost equal to an oxidation peak current and regardless of scan rate the reduction and oxidation peak potential is constant without any shift. In addition, it should be satisfied with the following relation,

$$\text{a. } \Delta E_p = E_{pa} - E_{pc} = 2.3\frac{RT}{nF}\ [mV]\ , \tag{2.7}$$

$$\text{b. } \left|E_p - E_{\frac{p}{2}}\right| = 2.3\frac{RT}{nF}\ [mV]\ . \tag{2.8}$$

The irreversible reaction is commonly founded as shown figure 2.10. This system is not satisfied with the Nernst equation when the electron transfer rate is slower than the mass transfer rate or CV is conducted at high scan rate. There is often no reverse peak. For the irreversible reaction, the number of electron with reaction, n, is related to the difference between the reduction peak potential, E_p, and the half reduction peak, $E_{p/2}$ like the following relation, [22]

$$\left|E_p - E_{\frac{p}{2}}\right| = 1.857\frac{RT}{n\alpha F}\ [mV]\ , \tag{2.9}$$

Where α is the transfer coefficient, it is generally assumed as 0.5. The diffusion coefficient can be calculated by using the Delahay equation, [23]

$$\frac{i_{pc}}{\sqrt{\nu}} = -0.4958nFSC\sqrt{\frac{n\alpha FD_{ox}}{RT}}\ . \tag{2.10}$$

And the reduction peak potential, E_p, have a relation with the apparent standard reduction potential, [19]

$$E_{pc} = E^{0*} - \frac{RT}{\alpha nF}[0.78 - \ln k_s + \ln(\sqrt{\frac{\alpha nF\nu D_{OX}}{RT}})] \qquad (2.11)$$

Eq. (2.11) is utilized to calculate the apparent reduction potential of Zr, Nb, Ni and Co in this dissertation.

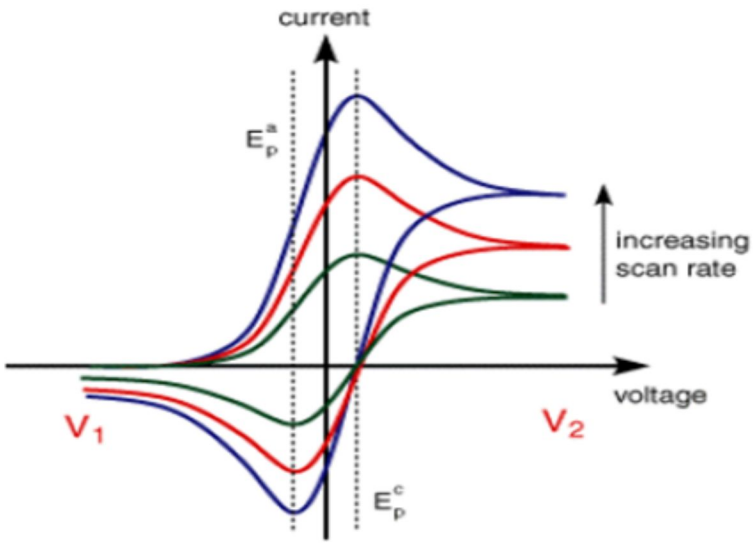

Figure 2.9 Cyclic voltammetry of the reversible reaction [22]

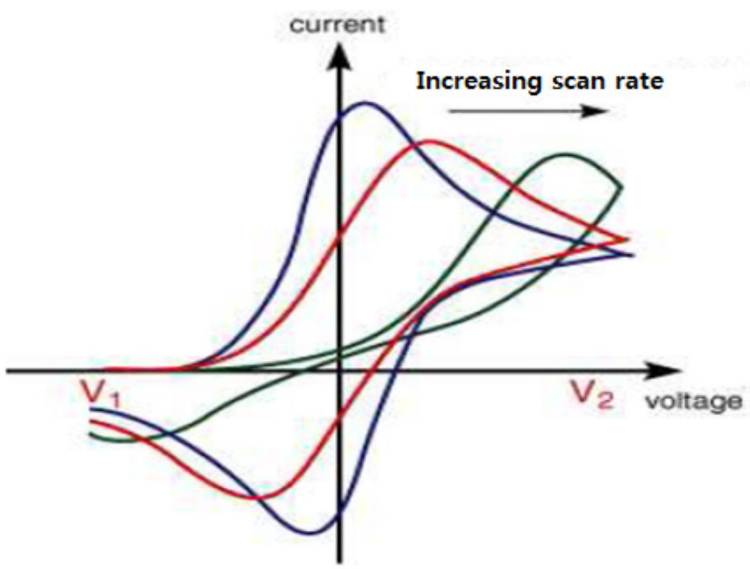

Figure 2.10 Cyclic voltammetry of the irreversible reaction [22]

3. Research Goal and Approach

3.1 Research Goal

The main goal of this dissertation is to determine a decontamination process to be needed for irradiated pressure tube based on electrorefiining in LiCl-KCl. To achieve the main goal, the following objectives are established. Zr and Nb electrochemical reactions among various oxidation states are very complicate and are not clarified yet. Therefore, one of the objectives is determining Zr and Nb redox mechanism in LiCl-KCl and carrying out electrorefining based on revealed redox behaviors. In addition to, Ni and Co redox mechanism in LiCl-KCl will be also determined, because Ni and Co are major radioactive nuclide in irradiated pressure tubes except Nb. The other object is verification for electrorefining experiment results with computational code. REFIN code, 1-D time dependent computational code developed by Seoul National University, was utilized to compare cathode deposition after electrorefining experiment.

Additional sub-goal are determining decontamination factor of Nb, Co, Ni and multistep number of electrorefining to be needed to exempt regulations or to be LLWs or VLLWs from ILWs.

Table 3.1 Radioactive waste level criteria of Nb^{94}, Co^{60}, Fe^{55}, Ni^{63}.

Element	LLW Specific Radioactivity (Bq/g)	VLLW Specific Radioactivity (Bq/g)	EW Sepecific Radioactivity (Bq/g)	DF needed to be EWs
Nb-94	$1.11x10^2$	10	0.1	$8.34x10^7$
Co-60	$3.70x10^7$	10	0.1	$2.37x10^8$
Fe-55	-	10^5	1000	$4.16x10^3$
Ni-63	$1.11x10^7$	10^4	100	$1.26x10^4$
Zr-93	-	-	10	Limited Recycle

3.2 Research Approach

To disposal of irradiated pressure tube at the LILW disposal repository in Kyoung-ju, partitioning long half-life or high specific radioactive nuclide such as Nb^{94}, Ni^{63}, Co^{60} from radioactive wastes of pressure tubes is needed. This result is revealed in Chapter 1. This dissertation focuses on separating Nb, Ni, Co from Zr-Nb alloys by conducting electrorefiing based on their redox potential differences in LiCl-KCl molten salts.

There is an approach flow chart of this study in shown figure 3.2. First-step is that CV experiments of key elements such as Zr, Nb, Ni, Co are conducted to determine their redox potentials. After checking their electrochemical behaviors, an applied potential at the cathode electrode is determined to separate only Zr. Second-step is that both of cathode deposition and precipitation in molten salts are analyzed by ICP-MS or XRD after electrorefining experiments. Concentration of each element is investigated by ICP-MS and compound forms are estimated by XRD. Through these processes, it can be checked for separating Nb, Co, Ni from Zr-Nb alloy. By using the results, decontamination factor of each element and the multi-step number of electrorefining can be determined, too. Next, computational electrorefining modeling is conducted by using electrorefining experiment conditions. To verify reliability of experiment, modeling results will compare to ICP-MS results. Finally, positive effect about economical and wastes management will be studied if recovered Zr through the electrorefining is recycled.

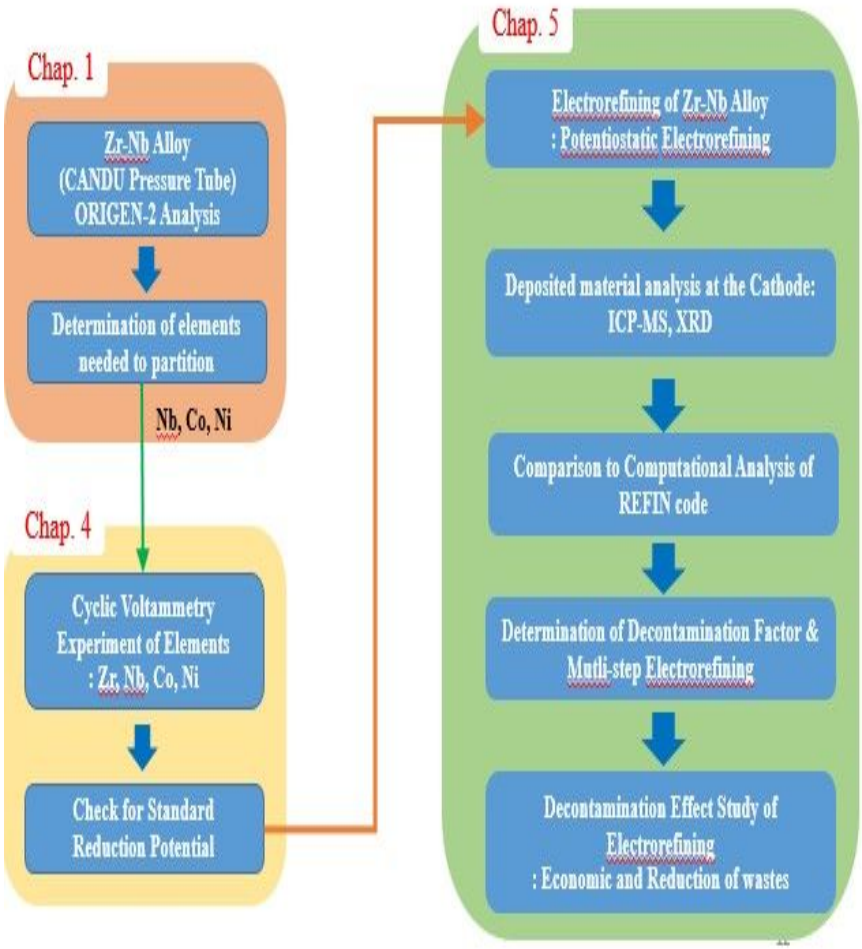

Figure 3.1 Flow Chart of Research Approach

4. Cyclic Voltammetry Experiment

4.1 Cyclic voltammetry of Zirconium in LiCl-KCl

To check zirconium redox behaviors, several CV experiments were conducted. Redox reactions that could occur in LiCl-KCl were determined based on previous electrolysis studies and peak behaviors according to scan rate, scan range and concentration of $ZrCl_4$.

4.1.1 Experiment Setup

Glove box filled with inert gas as shown in Figure 4.1 is used for all of the CV experiments using the LiCl-KCl. Used inert gas is Ar gas of 99.999% Oxygen and moisture concentrations were always monitored and maintained below 0.1 ppm during the CV experiments. A furnace and cell for CV experiment was installed as shown in Figure 4.2. A VersaStat3 potentiostat hardware and a VersaStudio software (ver. 2.44.4) were used to applied potential and current on the cell and provided analysis packages as shown in Figure 4.3. K-type thermocouple was used to measure the molten salt's temperature, and PID type heater controller was used to keep 500°C within ±1°C during experiments. Two quartz tubes with an inner diameter of 13mm and a height of 380 mm were equipped at the same cell for conducting CV experiment.

The working and counter electrodes were made of 99.99% purity tungsten wires with a diameter of 1mm obtained from the Sigma Aldrich and were inserted

with quartz guide tube with and inner diameter of 2mm. The reference electrode was used for the Ag/AgCl electrode, Ag electrode with a diameter of 1mm and purity of 99.99%, that was put within the LiCl-KCl-AgCl(1wt.%) solution. The purity of AgCl obtained from the Sigma Aldrich is 99.999%. The electrolyte was contained in a Pyrex tube with an inner diameter of 2mm and with one close-end. An anhydrous LiCl-KCl eutectic mixture with purity of 99.99% and an anhydrous ZrCl4 with purity of 99.99% were bought from the Sigma Aldrich, too.

To prepare low concentrations of $ZrCl_4$ in LiCl-KCl, LiCl-KCl-$ZrCl_4$(10 wt. %) was first prepared and then was diluted down to 0.2wt%, 0.5wt%, 1wt%, 2wt%, respectively. The mass of molten salt placed in the quartz tube for CV is about 3.0g. Each area of working and counter electrode was about 0.628cm^2.

Since Potentiostat used for CV experiments has limited current of 2A and as higher concentration, it is difficult to divide redox peak and redox current is much higher, it could not use the higher concentration solution. Scan rates set for experiments are various from 50mV/s to 1500mV/s. Low scan rate result (<500mV/s) is generally used to determine redox potential. And Scan range used for experiments is also various from -2.0V[vs. Ag/AgCl] to 1.0V[vs. Ag/AgCl]. Since chlorine ion could be oxidized to gas at about 1.2V[vs. Ag/AgCl], so it conducted all of the experiments under 1.2V[vs. Ag/AgCl].

Figure 4.1 Glove Box used to Cyclic Voltammetry experiments

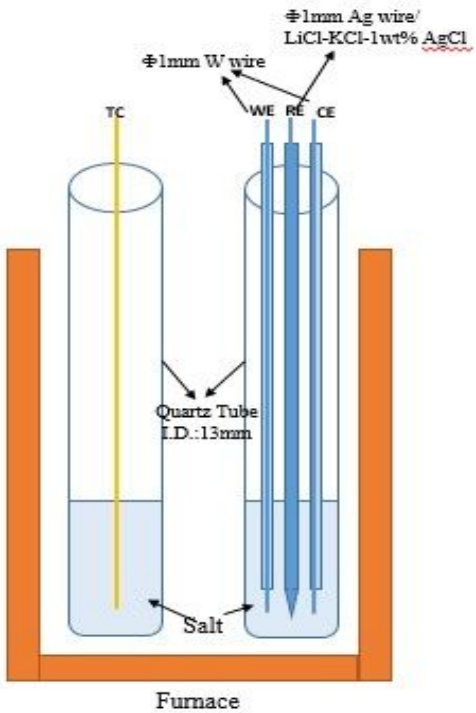

Figure 4.2 Cell and Furnace composition for CV experiment

Fig 4.3 PID heater and VersaSTAT3 Potentiometer

4.1.2 Cyclc Voltammetry results and Discussion

As shown in Figure 4.4, there were results of CV in the LiCl-KCl-$ZrCl_4$(1 wt. %) with a scan rate of 300 mV/s conducted for 11 different scan ranges. There were main 3 peaks of reduction (R1, R2, R3) and 4 peaks of oxidation (O1,O2, O3, O4). Since O1, O2 peaks were more sharply than O3 and O4, it was easy to separate O1, O2 from O3, O4. And it was easy to separate R2, R3 from R1 due to same reason. O1 peak was only seen in the the LiCl-KCl-$ZrCl_4$(0.2 wt. %). The higher concentration of $ZrCl_4$, O1 peak was overlapped with O2 peak, and so it was difficult to be noticeable. The identification of Zr redox peaks is as follow. Those of redox peaks were checked to compare with literature reviews in the Table 4.1[16]. There are exist some disagreements among the previous studies about the reduction behavior of Zr(IV) because of redox mechanism of Zr which has disproportionation in the LiCl-KCl molten salt.

O1 : $ZrCl \rightarrow Zr^{4+} + 3e^-$
O2 : $Zr \rightarrow Zr^{4+} + 4e^-$
O3 : $Zr(II) \rightarrow Zr(IV) + 2e^-$
O4 : $Zr(II)(monolayer) \rightarrow Zr(IV) + 2e^-$
$ZrCl(monolayer) \rightarrow Zr(IV) + 3e^-$
R1 : $Zr(IV) + 2e^- \rightarrow Zr(II)$
R2 : $Zr(IV) + 3e^- \rightarrow ZrCl$
R3 : $ZrCl + e^- \rightarrow Zr$

The more expansive the scan ranges were, the more increasing height of

oxidation and reduction peaks proportionally in the figure 4.4. O1 peak was seen when scan range was over -1.1V, however, it was not appeared when scan range was over -1.5V. Because O1 reaction is related to ZrCl and concentration of ZrCl in the narrow scan ranges was higher than scan ranges over -1.5V. R1, O3 reactions were soluble-soluble reactions, so these peaks were lower than other soluble-insoluble peaks and it was difficult to noticeable. And when scan range was over -1.5V, R3 peak appeared clearly. As R3 peak was shown, O1 peak was disappeared due to little concentration of ZrCl.

There are concentration effects on CV peaks from figure 4.4 to figure 4.7. At low concentration(0.2wt.%, 0.5wt.%) $ZrCl_4$, R3 peak was not shown in all scan rates. According to Yanqing Cai's study(2015), he thought that there may exist a competition between the reduction of Zr(IV) to Zr and ZrCl. At low Zr(IV) concentration, Zr(IV) is easy to be reduced to Zr instead of ZrCl. On the other hands, at high Zr(IV) concentration, Zr(IV) prefers to be reduced to ZrCl. This supports that O1 peak disappeared at low Zr(IV) concentration.

Table 4.1 Comparison of reaction identification for CV peaks in LiCl-KCl-$ZrCl_4$ in the literature [16].

Peak	Park (500°C, 1wt.% ZrCl4, tungsten electrode)[16]	Lee (500°C, 4wt.% ZrCl4, tungsten electrode) [12]	Ghosh (525°C, 1.84E-4mol/cm^3 ZrCl4, tungsten electrode) [24]	Sakamura (500°C, 0.00123mole fraction ZrCl4, tungsten electrode) [25]
O1	$ZrCl \rightarrow Zr(IV)+3e^-$ (major reaction) $ZrCl \rightarrow Zr(II)+e^-$	$ZrCl \rightarrow Zr(IV)+3e^-$ $Zr \rightarrow Zr(II)+2e^-$	$Zr \rightarrow Zr(I)+e^-$	$ZrCl \rightarrow Zr(IV)+3e^-$
O2	$Zr \rightarrow Zr(IV)+4e^-$ (major reaction) $Zr \rightarrow Zr(II)+2e^-$	$Zr \rightarrow Zr(IV)+4e^-$	$Zr \rightarrow Zr(II)+2e^-$ $Zr(I) \rightarrow Zr(II)+e^-$	$Zr \rightarrow Zr(IV)+4e^-$
O3	$Zr(II) \rightarrow Zr(IV)+2e^-$	$Zr(II) \rightarrow Zr(IV)+2e^-$	$Zr(II) \rightarrow Zr(IV)+2e^-$	Not observed
O4	$Zr(II)(monolayer) \rightarrow Zr(IV)+2e^-$ $ZrCl(monolayer) \rightarrow Zr(IV)+2e^-$	Not observed	Monolayer dissolution of Zr(II)	Not observed
R1	$Zr(IV)+2e^- \rightarrow Zr(II)$	$Zr(IV)+2e^- \rightarrow Zr(II)$	$Zr(IV)+2e^- \rightarrow Zr(II)$	$Zr(IV)+2e^- \rightarrow Zr(II)$
R2	$Zr(IV)+3e^- \rightarrow ZrCl$ (major reaction) $Zr(II)+e^- \rightarrow ZrCl$	$Zr(II)+2e^- \rightarrow Zr$ $Zr(IV)+3e^- \rightarrow ZrCl$	$Zr(II)+2e^- \rightarrow Zr$ $Zr(II)+e^- \rightarrow Zr(I)$ $Zr(I)+e^- \rightarrow Zr$	$Zr(IV)+4e^- \rightarrow Zr$ $Zr(IV)+3e^- \rightarrow ZrCl$
R3	$ZrCl+e^- \rightarrow Zr$ (major reaction) $Zr(II)+2e^- \rightarrow Zr$ $Zr(IV)+4e^- \rightarrow Zr$	$ZrCl+e^- \rightarrow Zr$ $Zr(IV)+4e^- \rightarrow Zr$	Not observed	$ZrCl+e^- \rightarrow Zr$

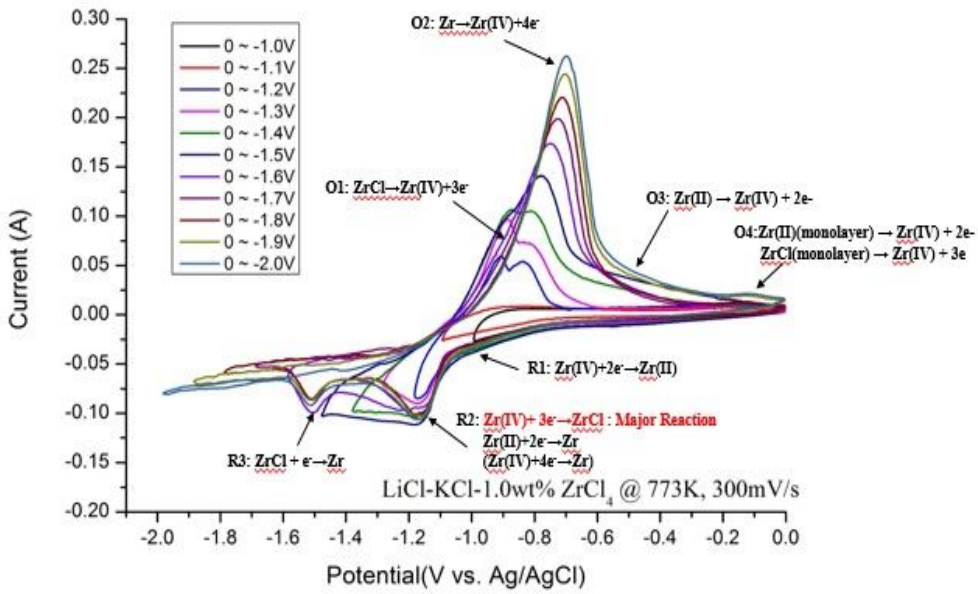

Figure.4.4 Cyclic voltammetry with the major reaction which could contribute to each peak according to scan range for the scan rate of 300 mV/s in 500°C LiCl-KCl-$ZrCl_4$(1 wt.%)

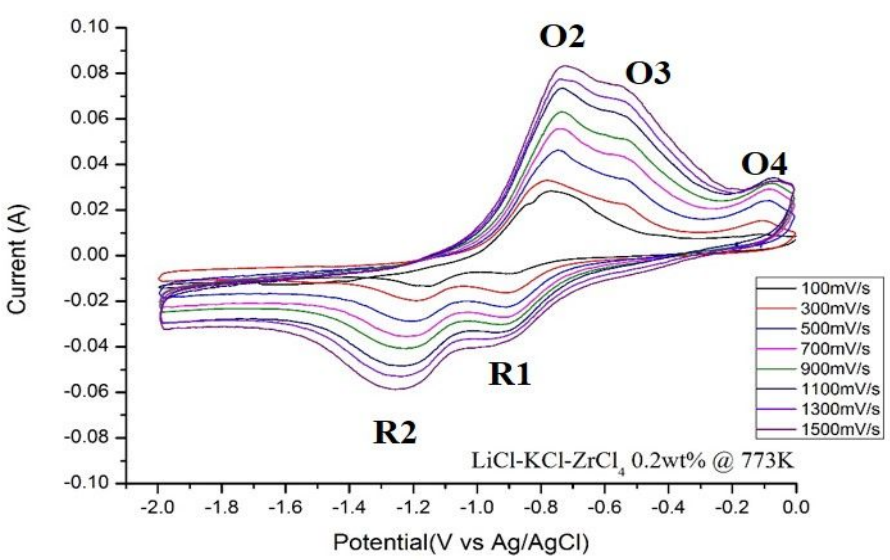

Figure 4.5 Cyclic voltammetry s according to scan rate for the scan range from 0 to -2.0V (vs. 1 wt. % Ag/AgCl) in 500°C LiCl-KCl-$ZrCl_4$(0.2 wt. %)

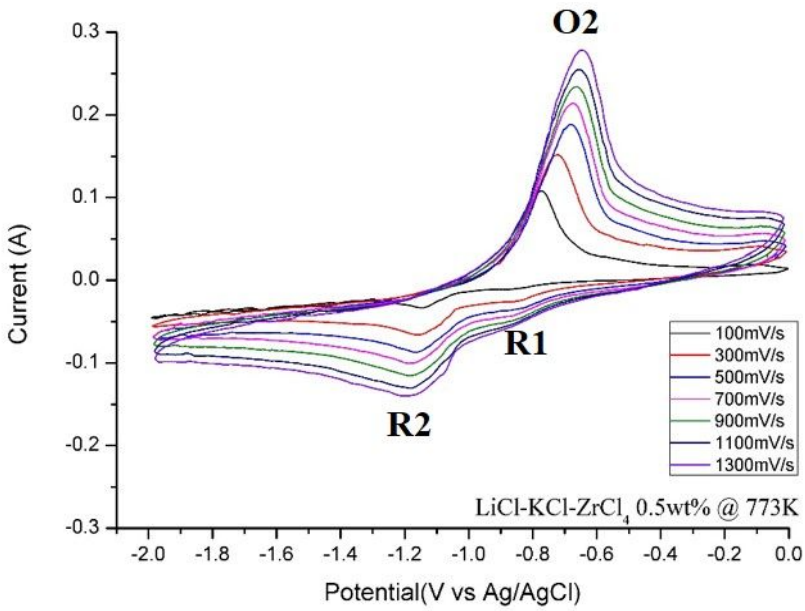

Figure 4.6 Cyclic voltammetry according to scan rate for the scan range from 0 to -2.0V (vs. 1 wt. % Ag/AgCl) in 500°C LiCl-KCl-$ZrCl_4$(0.5 wt. %)

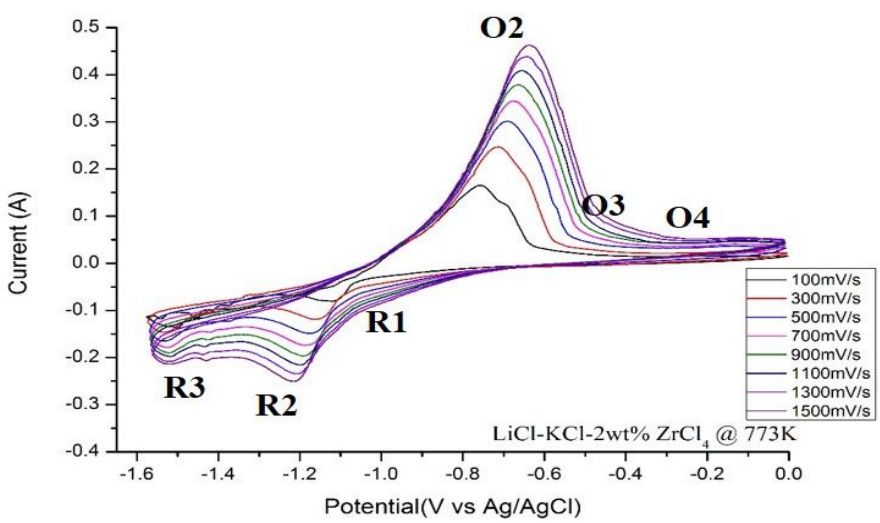

Figure 4.7 Cyclic voltammetry according to scan rate for the scan range from 0 to -2.0V (vs. 1 wt. % Ag/AgCl) in 500°C LiCl-KCl-$ZrCl_4$(2.0 wt. %)

Cyclic Voltammetry of Zr is irreversible due to asymmetric shape between oxidation peak and reduction peak. For this reason, we can determine apparent reduction potential of each reduction peak by using following relation, where, E_{pc} is the peak potential, E^{0*} is the apparent reduction potential, R is the universal gas constant(8.314J/mol/K), T is the absolute temperature, α is the transfer coefficients, n is the number of electron participating in the reaction, F is the Faraday's constant(96,485 C/mol), k_s is the standard rate constant, ν is the scan rate, and D_{ox} is the diffusion coefficient[21].

It is assumed that α is 0.5 and k_s is 2.6×10^{-4}.

$$E_{pc} = E^{0*} - \frac{RT}{\alpha nF}[0.78 - \ln k_s + \ln(\sqrt{\frac{\alpha nF\nu D_{OX}}{RT}})] \qquad (4.1)$$

Each apparent reduction potential is shown as from Table 4.1 and when it compare to previous study values, they are almost same. So we think that the CV results of Zr in LiCl-KCl is well reliable.

Table 4.2 Zr(II)↔Zr(0) apparent reduction potential result of this study as concentration

Concentration (wt.% $ZrCl_4$)	Zr(IV)/Zr(0) Apparent Standard Reduction Potential (V vs. Ag/AgCl)@0.1V/Sec
2.0	-1.137
1.0	-1.086
0.5	-1.138
0.2	-1.136
Average	-1.124

Table 4.3 Zr(II)↔Zr(0) Literature Review values

Reference	Zr(IV)/Zr(0) Apparent Standard Reduction Potential (V vs. Ag/AgCl)@0.1V/Sec
[1]	-1.266
[2]	-1.120
[3]	-1.020
[4]	-1.007

Ref. [1] R.O.Hoover, Ph.D Thesis, 2014 [21].
[2] R.Baboian, et al., Electrochemical Studies on Zirconium and Hafnium in Molten LiCI-KCI Eutectic, 1965 [26].
[3] CRIEPI report T93033, Pyrometallurgy Data Book, 1994 [27].
[4] J.A.Planmbeck, et al., Electromtive force series in molten salts, 1967 [28].

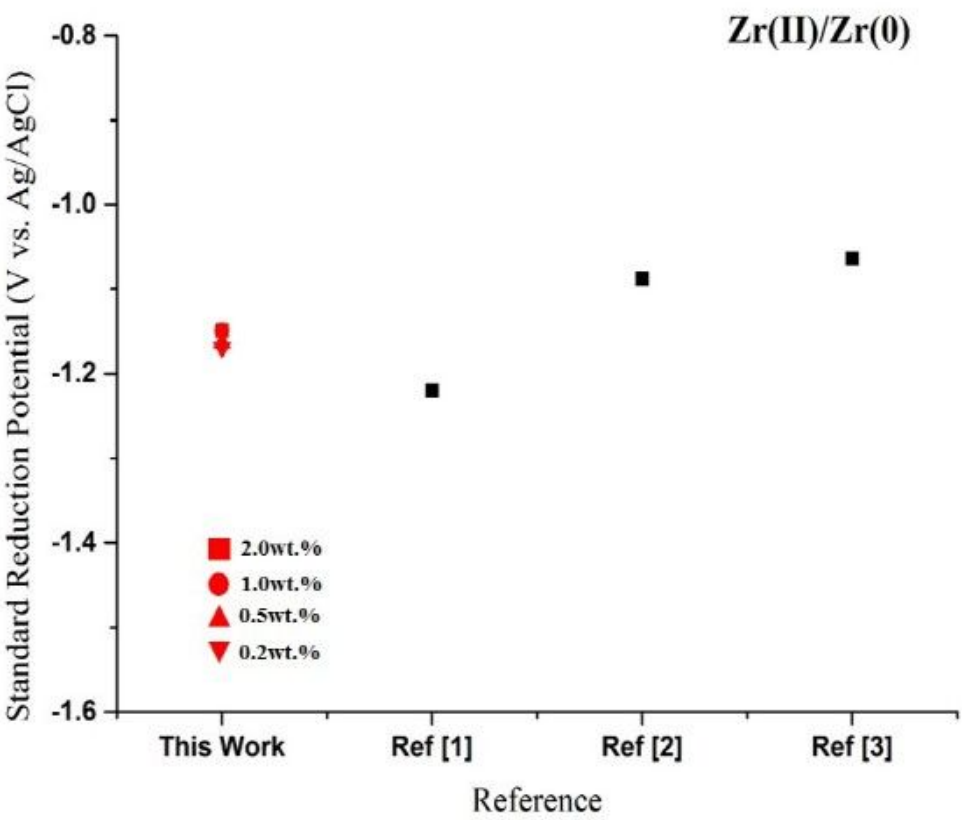

Figure 4.8 Zr(II)↔Zr(0) redox potential comparison to previous studies

Table 4.4 Zr(IV)↔Zr(0) apparent reduction potential result of this study as concentration

Concentration (wt.% $ZrCl_4$)	Zr(IV)/Zr(0) Apparent Standard Reduction Potential (V vs. Ag/AgCl)@0.1V/Sec
2.0	-1.149
1.0	-1.149
0.5	-1.164
0.2	-1.169
Average	-1.159

Table 4.5 Zr(IV)↔Zr(0) Literature Review values

Reference	Zr(IV)/Zr(0) Apparent Standard Reduction Potential (V vs. Ag/AgCl)@0.1V/Sec
[1]	-1.220
[2]	-1.088
[3]	-1.064

Ref. [1] R.Baboian, et al., Electrochemical Studies on Zirconium and Hafnium in Molten LiCI-KCI Eutectic, 1965 [26].
[2] Bard, et al., Encyclodepia of electrochemistry of the elelmet Vol X. 1976[18].
[3] J.A.Planmbeck, et al., Electromtive force series in molten salts, 1967 [28].

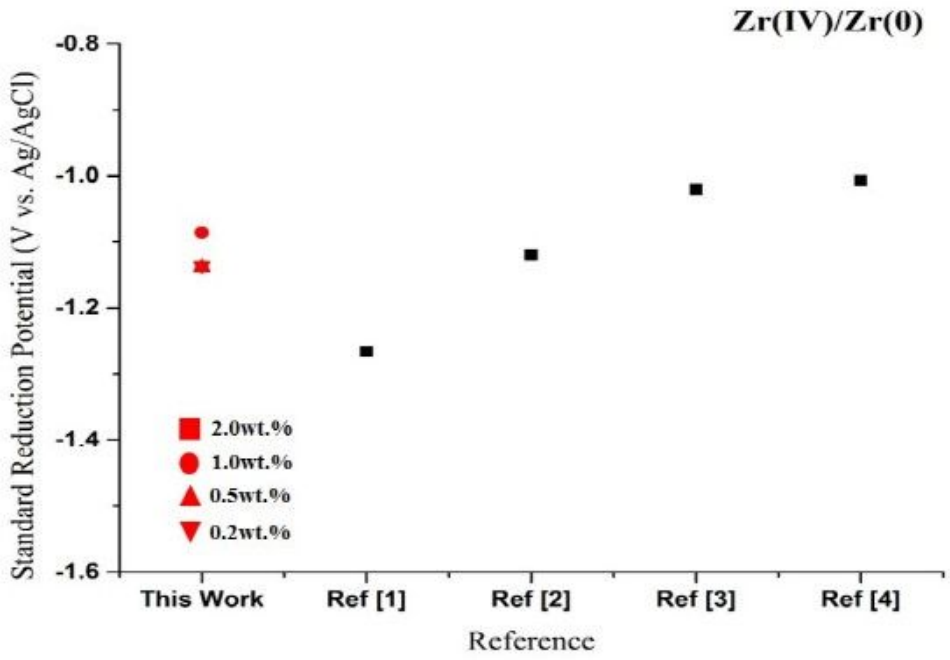

Figure 4.9 Zr(IV)↔Zr(0) redox potential comparison to previous studies

Table 4.6 Zr(IV)↔Zr(II) apparent reduction potential result of this study as concentration

Concentration (wt.% $ZrCl_4$)	Zr(IV)/Zr(0) Apparent Standard Reduction Potential (V vs. Ag/AgCl)@0.1V/Sec
0.2	-0.906

Table 4.7 Zr(IV)↔Zr(II) Literature Review values

Reference	Zr(IV)/Zr(II) Apparent Standard Reduction Potential (V vs. Ag/AgCl)@0.1V/Sec
[1]	-0.982
[2]	-0.737
[3]	-0.951
[4]	-1.121

Ref. [1] R.O.Hoover, Ph.D Thesis, 2014 [21].
[2] M.Simpson et al., Investigation of electrochemical recovery of zirconium from spent nuclear fuels, 2014 [29]
[3] CRIEPI report T93033, Pyrometallurgy Data Book, 1994 [27]
[4] J.A.Planmbeck et al., Electromtive force series in molten salts, 1967 [28]

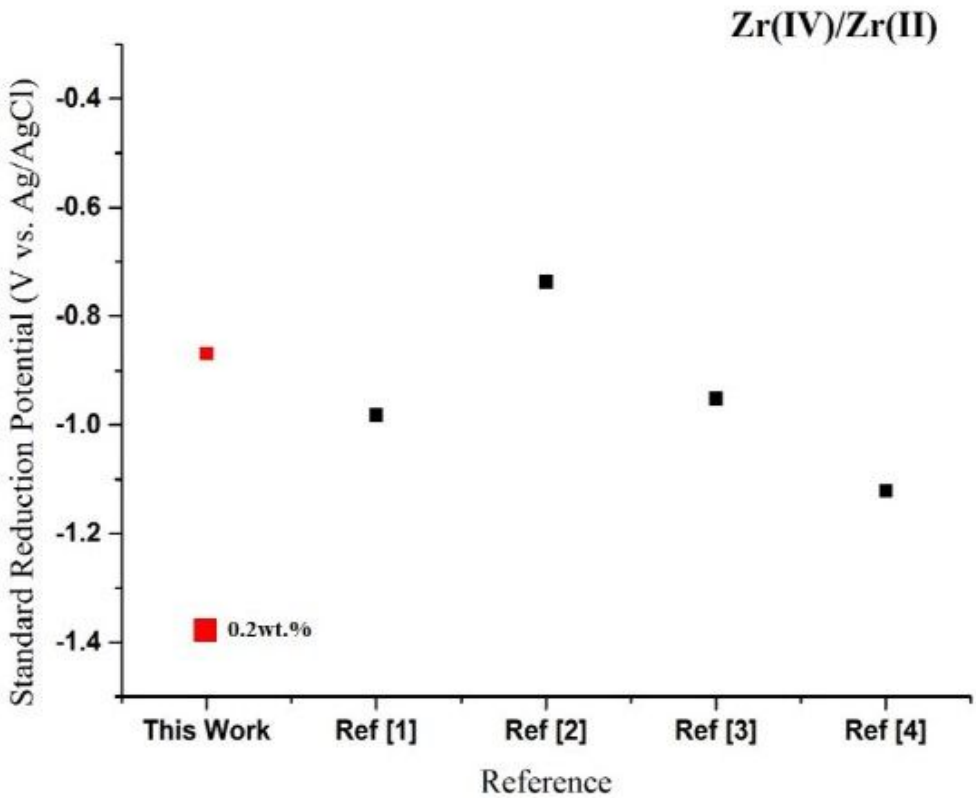

Figure 4.10 Zr(IV)↔Zr(II) redox potential comparison to previous studies

4.2 Cyclic voltammetry of Niobium in LiCl-KCl

To check niobium redox behavior, several CV experiments were conducted. Redox reactions that could occur in LiCl-KCl were determined based on previous electrolysis studies and peak behaviors according to scan rate, scan range and concentration of $NbCl_5$.

4.2.1 Experimental Setup

CV experimental setup on Nb such as the used equipment, electrode, cell, the operating temperature, and so on, is equal to CV experimental conditions for Zr as written in section of 4.1.1. An anhydrous LiCl-KCl eutectic mixture with purity of 99.99% was obtained from the Sigma Aldrich, and anhydrous $NbCl_5$ with purity of 99.95% were supplied from the Alpha Aesar. Molten salts of four different concentration(1wt.% ~ 0.1wt.%) for each chloride were utilized for CV in the electrochemical cell. To handle small amount of reagents, molten salt solutions of 6 wt. % were first prepared and they were diluted down to the concentration required for CVs. The mass of molten salt contained in the quartz test tube for CV is 3.0g. Each area of counter electrode and working electrode was 0.628 cm^2.

The boiling point of Nb is lower than the melting point of LiCl-KCl eutectic salts. So concentration of prepared LiCl-KCl-$NbCl_5$ is measured by ICP-MS. When it was prepared, initially the weight percentage (wt.%) of $NbCl_5$ was about 10wt.% but the result of ICP-MS for prepared LiCl-KCl-$NbCl_5$ was about 6wt%. Relatively

much $NbCl_5$ was evaporated during preparing samples.

4.2.2 Cyclc Voltammetry results and Discussion

As shown in Figure 4.11, there were results of CV in the LiCl-KCl-$NbCl_5$(3.2 wt. %) with six scan rates from 50 mV/s to 900 mV/s conducted for the scan range from 1.1V (vs. Ag/AgCl) to -0.9 (vs. Ag/Ag/Cl). There are 6 peaks of reduction (R1, R2, R3, R4, R5, R6) and 4 peaks of oxidation (O1,O2, O3, O4). Since O1, O2 peaks are more sharply than O3 and O4, it is easy to separate O1, O2 from O3, O4. And it was easy to separate R1, R2, R4 from the others due to same reason. R6 peak was only seen in the the LiCl-KCl-$NbCl_5$(3.2wt. %).

The identification of Nb redox peaks is as follows. Those of redox peaks were checked to compare with literature reviews. .[Nb 논문목록]

O1 : $Nb^{2+} \rightarrow Nb^{3+} + e^-$

O2 : $Nb \rightarrow Nb^{3+} + 3e^-$

O3 : $Nb^{3+} \rightarrow Nb^{4+} + e^-$

O4 : $Nb^{4+} \rightarrow Nb^{5+} + e^-$

R1 : $Nb^{5+} + e- \rightarrow Nb^{4+}$

R2 : $Nb^{4+} + e- \rightarrow Nb^{3+}$

R3 : $Nb^{3+} + 3e- \rightarrow Nb$

R4 : $Nb^{3+} + e- \rightarrow Nb^{2+}$

R5 : $mNb^{3+} + ye- \rightarrow NbCl_n$ (n:2~3) ; Nb subchloride reduction

R6 : $Nb^{2+} + 2e- \rightarrow Nb$

There are exist some disagreements among the previous studies about the

reduction behavior of Nb because redox mechanism of Nb has disproportionation in the LiCl-KCl molten salt like Zr. The redox behaviors of Nb are more complex than Zr. According to Lantelme's study[30], Nb makes a subchloride in chloride molten salts and at the temperature over 650°C, main dominant subchloride Nb_3Cl_8 is disproportionated into Nb and $NbCl_4$, so CV result of Nb at 630°C was very simpler than others at the low temperature. That is, there were no R5 and R6 peaks at in Lantelme's study .The solubility of Nb_3Cl_8 in LiCl-KCl can't exceed 0.5wt.% at 500°C according to M.Mohamedi's study[31]. R5 and R6 peaks in figure 4.11 and figure 4.14 were assessed by Nb_3Cl_8, because these peaks were not shown in the lower concentration of $NbCl_5$ than 0.5wt.% of $NbCl_5$. R6 peak was revealed in only figure 4.11, it is thought that Nb_3Cl_8 was reduced as two steps like M.Mohamedi's study. He insisted that Nb(III) was reduced into Nb(II) in the first reduction step and next step Nb(II) was reduced into Nb.

The higher concentration of $NbCl_5$, O3 peak was seen as the shoulder near O2 peak, and so it was difficult to be noticeable. It is difficult to distinguish R5 peak due to reduction reactions of Nb subchloride.

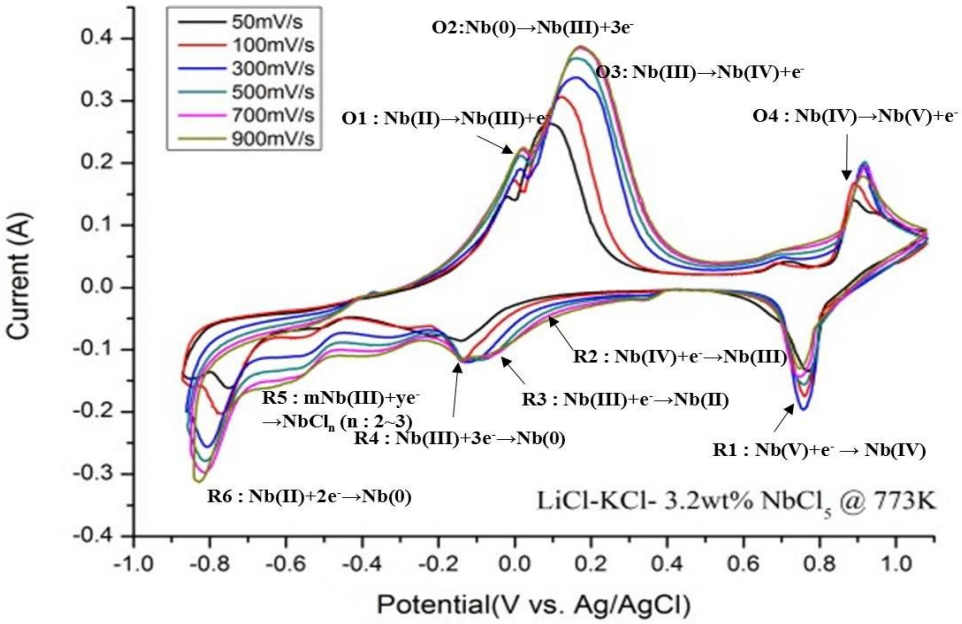

Figure 4.11 Cyclic voltammetry according to scan rate for the scan range from 1.1 to -0.9V (vs. 1 wt. % Ag/AgCl) in 500°C LiCl-KCl-$NbCl_5$(3.2 wt. %)

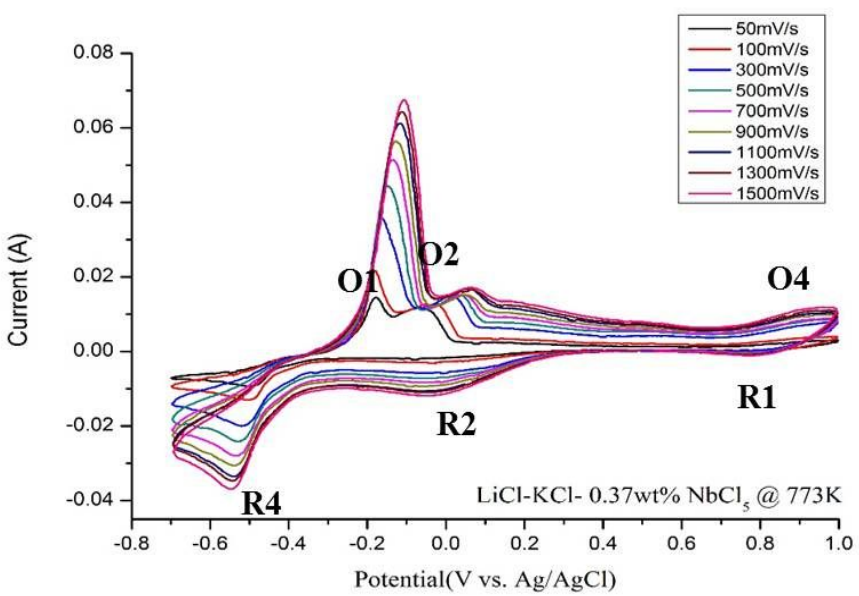

Figure 4.12 Cyclic voltammetry according to scan rate for the scan range from 1.0 to -0.7V (vs. 1 wt. % Ag/AgCl) in 500°C LiCl-KCl-$NbCl_5$(0.37 wt. %)

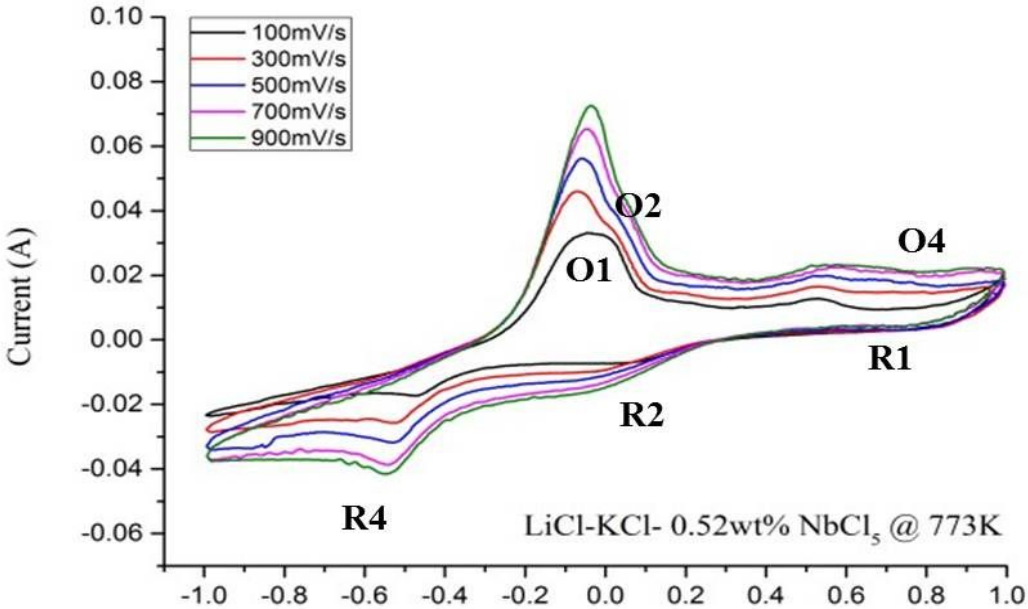

Figure 4.13 Cyclic voltammetry according to scan rate for the scan range from 1.0 to -0.1V (vs. 1 wt. % Ag/AgCl) in 500°C LiCl-KCl-$NbCl_5$(0.52 wt. %)

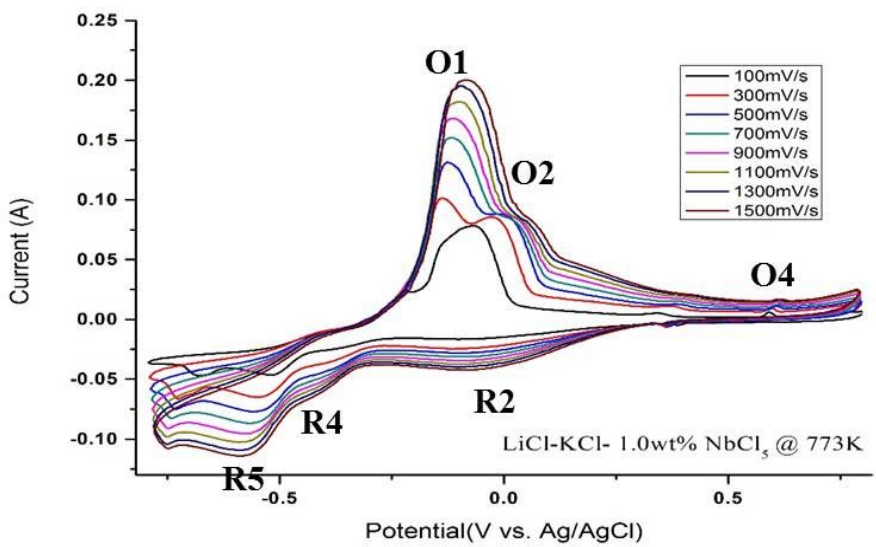

Figure 4.14 Cyclic voltammetry according to scan rate for the scan range from 0.8 to -0.8V (vs. 1 wt. % Ag/AgCl) in 500°C LiCl-KCl-$NbCl_5$(1.0 wt. %)

Table 4.8 Nb(III)↔Nb(0) apparent reduction potential result of this study as concentration

Concentration (wt.% $NbCl_5$)	Nb(III)/Nb(0) Apparent Standard Reduction Potential (V vs. Ag/AgCl)@0.1V/Sec
3.2	-0.160
1.0	-0.547
0.52	-0.515
0.37	-0.531
Average	-0.438

Table 4.9 Nb(III)↔Nb(0) Literature Review values

Reference	Nb(III)/Nb(0) Apparent Standard Reduction Potential (V vs. Ag/AgCl)@0.1V/Sec
[1]	-0.520
[2]	-0.430
[3]	-0.154
[4]	-0.254
[5]	-0.189

Ref. [1] R.Fujita, et al., Development of a Zirconium Recycle Process from Zircaloy Waste of a BoilingWater Reactor (BWR), 2005 [15].
[2] Bard, et al., Encyclodepia of electrochemistry of the element Vol X. 1976[18].
[3] F.Lantelme, et al., Cyclic voltammetry at a metallic electrode,1994[32].
[4] F.Lantelme, et al., Electrochemical behavior of solutions of niobium chlorides in fused alkali chlorides, 1993 [30].
[5] F.Lantelme, et al., Niobium and titanium electrowinning in fused salts, 2010 [33].

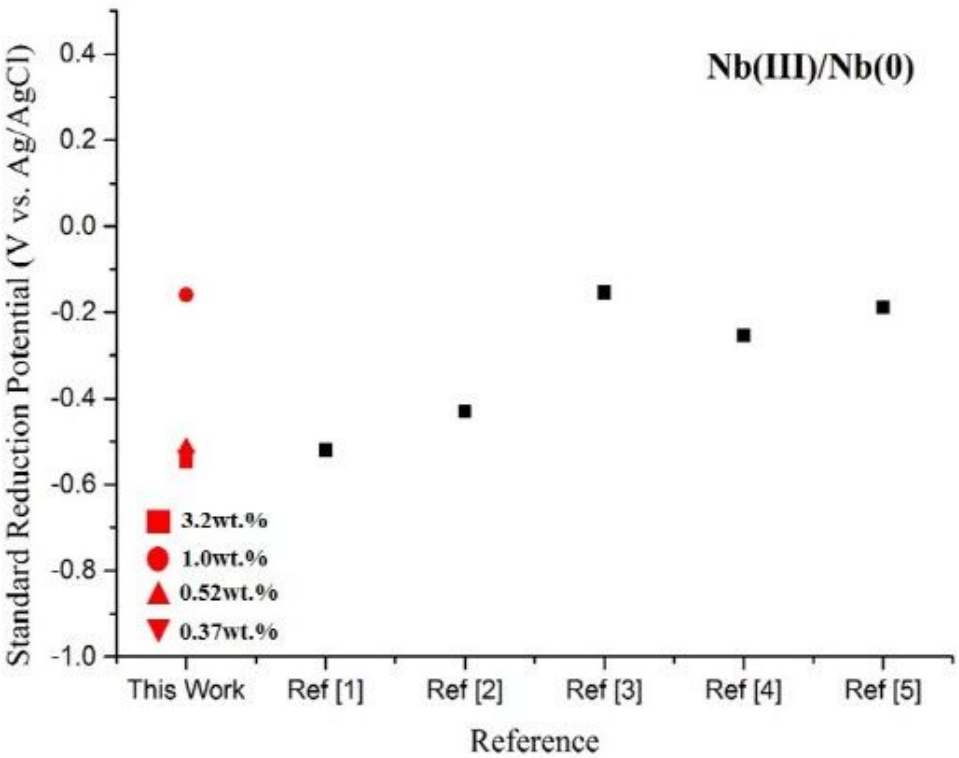

Figure 4.15 Nb(III)↔Nb(0) redox potential comparison to previous studies

4.3 Cyclic voltammetry of Nickel and Cobalt in LiCl-KCl

To check nickel and cobalt redox behavior, several CV experiments were conducted. Redox reactions that could occur in LiCl-KCl were determined based on previous electrolysis studies and peak behaviors according to scan rate, scan range and concentration of $NiCl_2$ and $CoCl_2$.

4.3.1 Experiment Setup

CV experimental setups on Ni and Co are same as experiments for Zr Cyclic voltammetry study as shown in section of 4.1.1. An anhydrous LiCl-KCl eutectic mixture with purity of 99.99% and an anhydrous $NiCl_2$ and $CoCl_2$ with purity of 99.99% were bought from the Sigma Aldrich. Molten salts of four different concentration(1wt.% ~ 0.1wt.%) for each chloride were utilized for CV in the electrochemical cell. Since Ni and Co play roles as impurities in the irradiated pressure tube, their concentration of the CV experiment is lower than Zr or Nb condition. Molten salt solutions of 10 wt. % were first prepared and they were diluted down to the concentration required for CVs. The mass of molten salt contained in the quartz test tube for CV is 3.0g. Each area of counter electrode and working electrode was 0.628 cm^2.

4.3.2 Cyclc Voltammetry results and Discussion

Solutions' concentrations are respectively 0.1, 0.2, 0.5 and 1.0 wt. % $NiCl_2$, $CoCl_2$ salts. These results are shown in from the figure 4.16 to the figure 4.25 respectively.

Only single oxidation and reduction peaks were observed for all concentration as literature studies. Each apparent reduction potential is calculated by using Eq. (4.1) and results of Ni and Co are represented in table 4.9 and table 4.11 respectively.

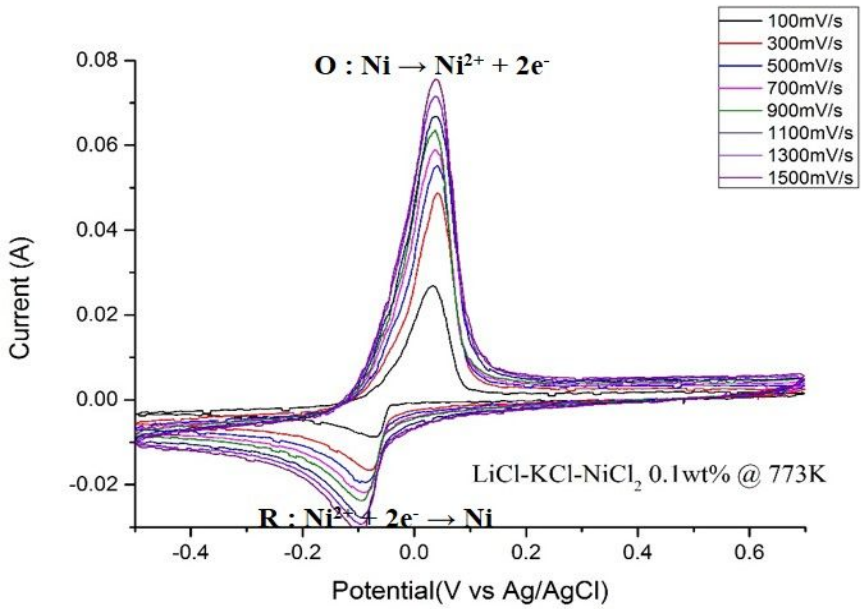

Figure 4.16 Cyclic voltammetry according to scan rate for the scan range from 0.7 to -0.5V (vs. 1 wt. % Ag/AgCl) in 500°C LiCl-KCl-$NiCl_2$(0.1wt. %)

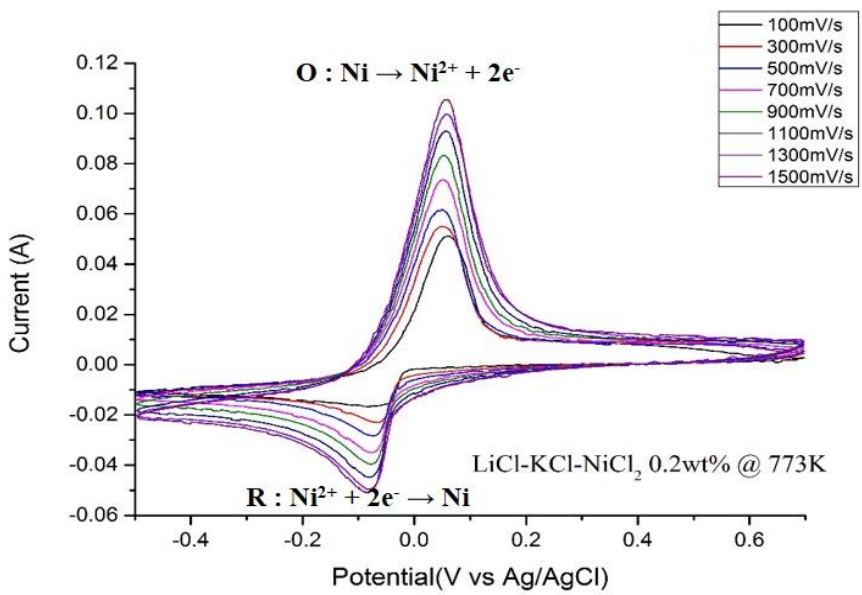

Figure 4.17 Cyclic voltammetry according to scan rate for the scan range from 0.7 to -0.5V (vs. 1 wt. % Ag/AgCl) in 500°C LiCl-KCl-$NiCl_2$(0.2 wt. %)

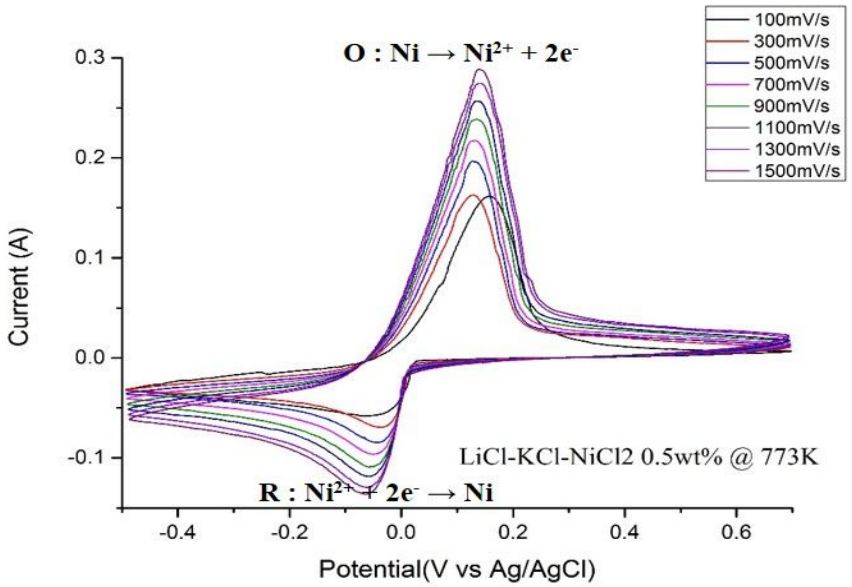

Figure 4.18 Cyclic voltammetry according to scan rate for the scan range from 0.7 to -0.5V (vs. 1 wt. % Ag/AgCl) in 500°C LiCl-KCl-$NiCl_2$(0.5 wt. %)

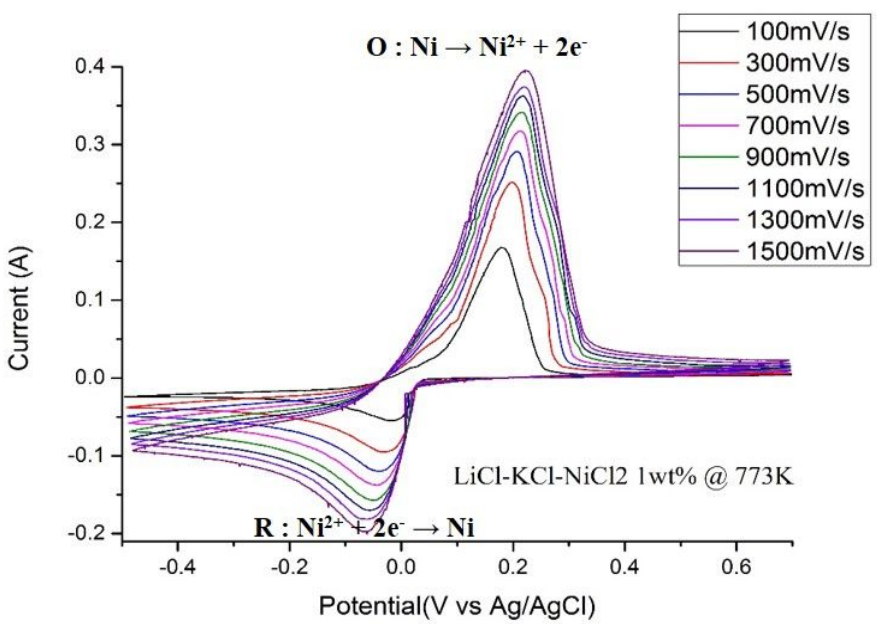

Figure 4.19 Cyclic voltammetry according to scan rate for the scan range from 0.7 to -0.5V (vs. 1 wt. % Ag/AgCl) in 500°C LiCl-KCl-$NiCl_2$(1.0 wt. %)

Table 4.10 Ni(II)↔Ni(0) apparent reduction potential result of this study as concentration

Concentration (wt.% $NiCl_2$)	Ni(II)/Ni(0) Apparent Standard Reduction Potential (V vs. Ag/AgCl)@0.1V/Sec
1.0	-0.059
0.5	-0.047
0.2	-0.084
0.1	-0.069
Average	-0.065

Table 4.11 Ni(II)↔Ni(0) Literature Review values

Reference	Ni(II)/Ni(0) Apparent Standard Reduction Potential (V vs. Ag/AgCl)@0.1V/Sec
[1]	-0.106
[2]	-0.070
[3]	-0.052
[4]	-0.068

Ref. [1] W.K.Behl et al., Linear Sweep Voltammetry of Ni(ll),Co(ll), Cd(ll), and Pb(ll) at Glassy Carbon Electrodes in Molten Lithium Chloride-Potassium Chloride Eutectic, 1971 [34].

[2] K.E.Johnson, et al., Advances in molten salts chemistry, Chap. 3, 1973[35].

[3] H.A.Laitinen et al., An Electromotive Force Series in Molten Lithium Chloride-Potassium Chloride Eutectic, 1958 [36].

[4] Bard, et al., Encyclodepia of electrochemistry of the element Vol X., 1976 [18].

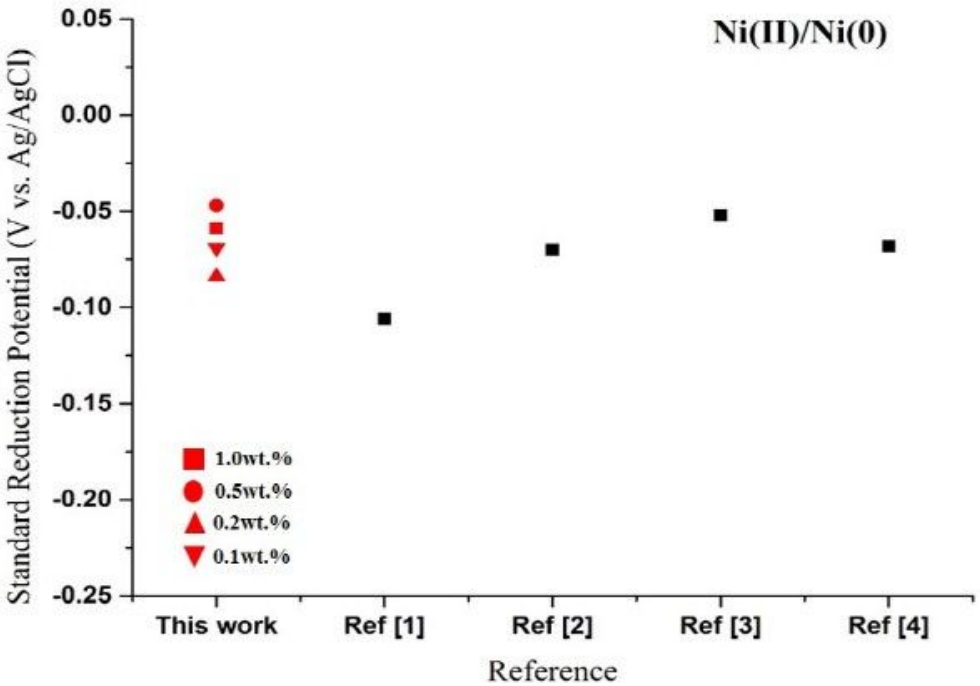

Figure 4.20 Ni(II)↔Ni(0) redox potential comparison to previous studies

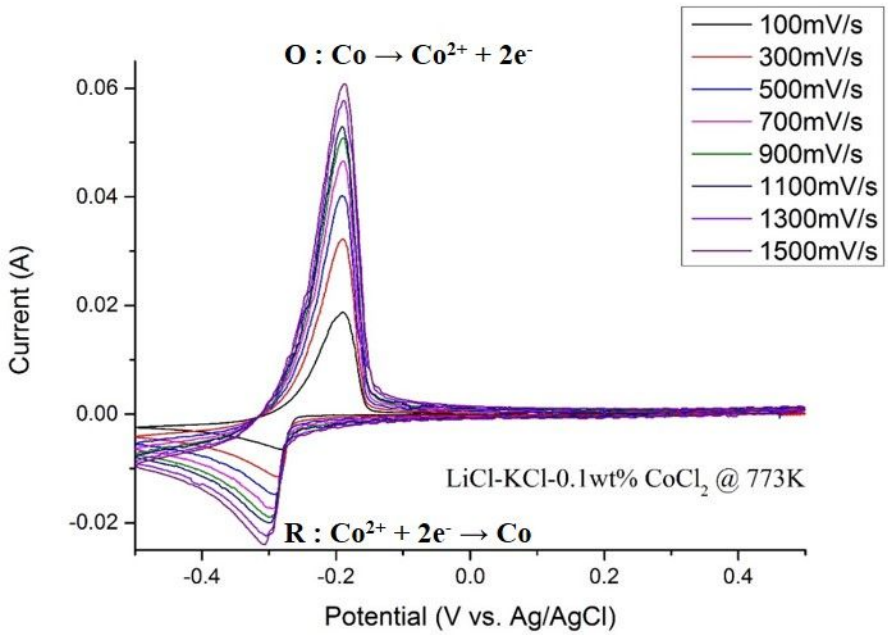

Figure 4.21 Cyclic voltammetry according to scan rate for the scan range from 0.5 to -0.5V (vs. 1 wt. % Ag/AgCl) in 500°C LiCl-KCl-$CoCl_2$(0.1 wt. %)

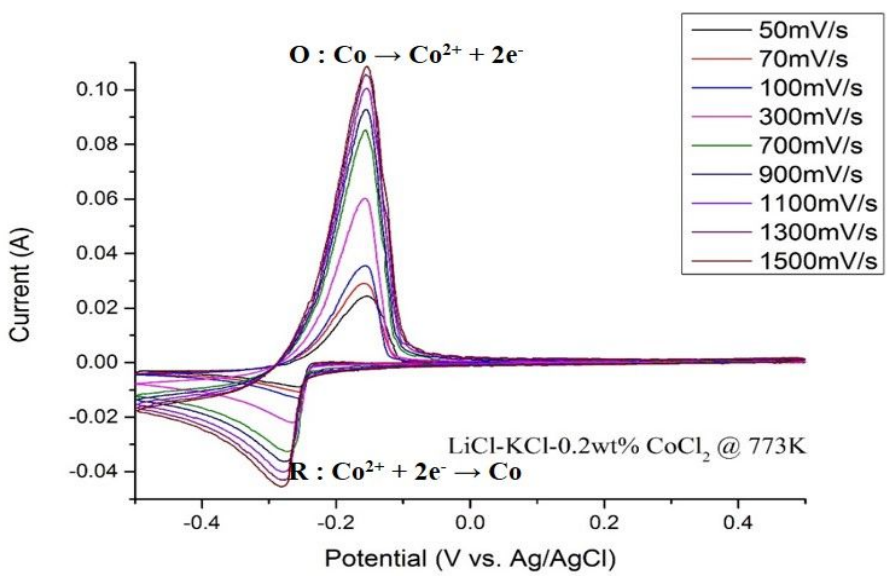

Figure 4.22 Cyclic voltammograms according to scan rate for the scan range from 0.5 to -0.5V (vs. 1 wt. % Ag/AgCl) in 500°C LiCl-KCl-$CoCl_2$(0.2 wt. %)

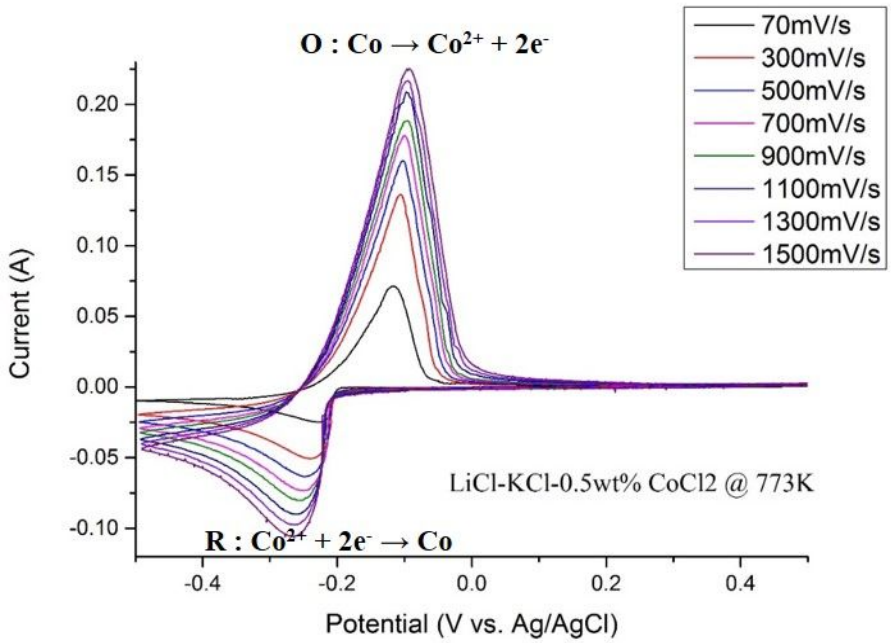

Figure 4.23 Cyclic voltammograms according to scan rate for the scan range from 0.5 to -0.5V (vs. 1 wt. % Ag/AgCl) in 500°C LiCl-KCl-$CoCl_2$(0.5 wt. %)

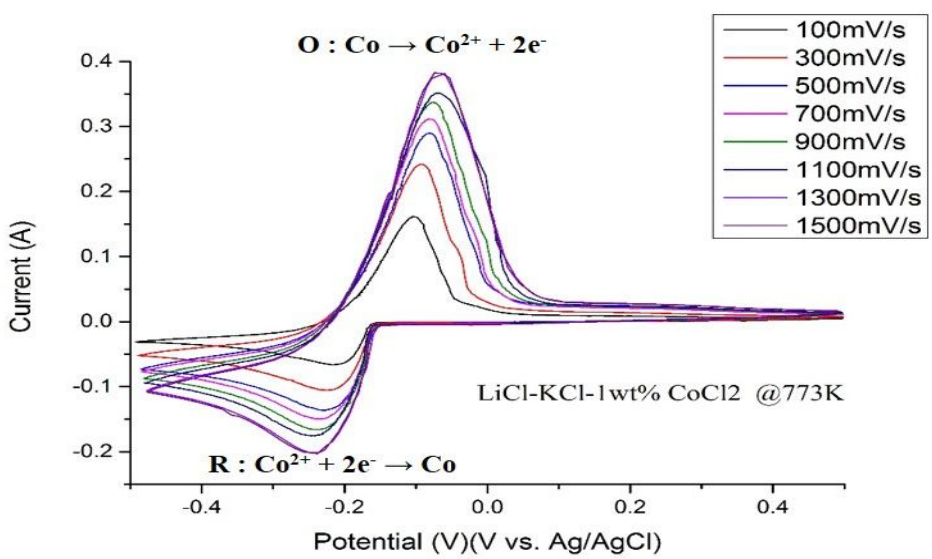

Figure 4.24 Cyclic voltammograms according to scan rate for the scan range from 0.5 to -0.5V (vs. 1 wt. % Ag/AgCl) in 500°C LiCl-KCl-$CoCl_2$(1.0 wt. %)

Table 4.12 Co(II)↔Co(0) apparent reduction potential result of this study as concentration

Concentration (wt.% $CoCl_2$)	Co(II)/Co(0) Apparent Standard Reduction Potential (V vs. Ag/AgCl)@0.1V/Sec
1.0	-0.239
0.5	-0.265
0.2	-0.275
0.1	-0.301
Average	-0.270

Table 4.13 Co(II)↔Co(0) Literature Review values

Reference	Co(II)/Co(0) Apparent Standard Reduction Potential (V vs. Ag/AgCl)@0.1V/Sec
[1]	-0.262
[2]	-0.241
[3]	-0.264
[4]	-0.248

Ref. [1] W.K.Behl et al., Linear Sweep Voltammetry of Ni(ll),Co(ll), Cd(ll), and Pb(ll) at Glassy Carbon Electrodes in Molten Lithium Chloride-Potassium Chloride Eutectic, 1971[34].
[2] H.A.Laitinen et al., Chronopotentiometry in fused LiCl-KCl, 1958[37].
[3] Bard, et al., Encyclodepia of electrochemistry of the element Vol X., 1976 [18].
[4] H.A.Laitinen et al., An Electromotive Force Series in Molten Lithium Chloride-Potassium Chloride Eutectic, 1958 [36]

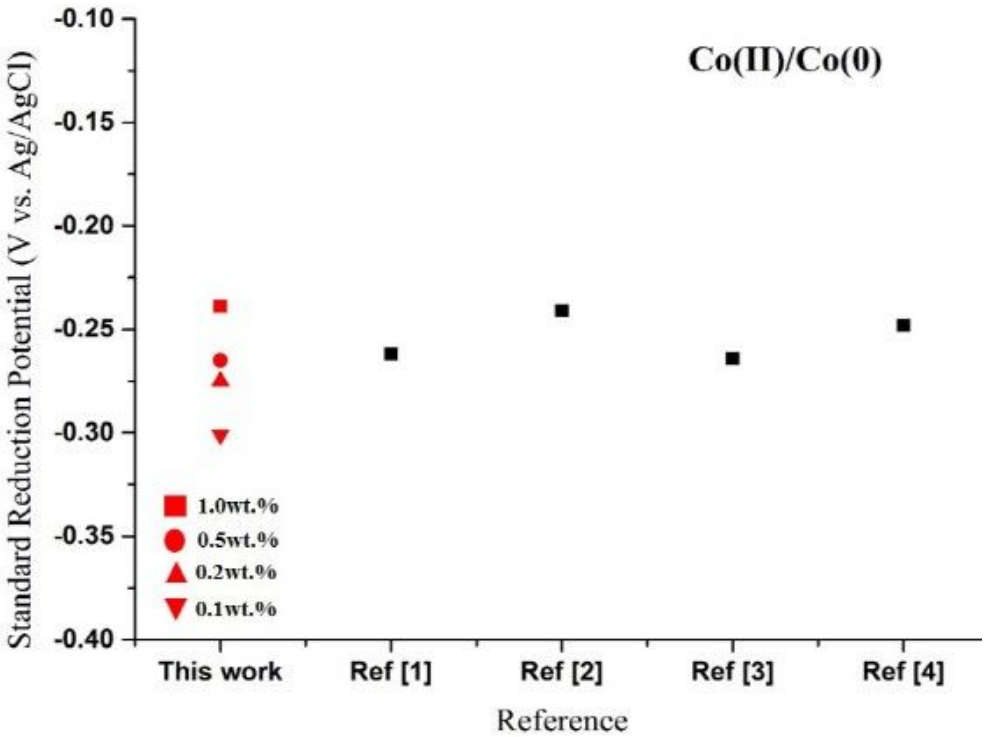

Figure 4.25 Co(II)↔Co(0) redox potential comparison to previous studies

5. Electrorefining experiments of Zr-Nb Alloys

5.1 Experimental setup

Electrorefining of Zr-Nb alloys were conducted by using the CV experimental setup. Electrorefining cell consisted as shown in Figure 5.2. Used inert gas in the glove box is Ar gas of 99.999% Oxygen and moisture concentrations were always monitored and maintained below 0.1 ppm during the elecrorefining experiments. Quartz tube with an inner diameter of 27 mm, an outer diameter of 30 mm and a height of 380 mm was utilized. Tungsten rod with a diameter of 3.175 mm and purity of 99.95% obtained from Alfa Aessa was used for a cathode. Zr metal is harder to deposit cathode than ZrCl. So Tungsten electrode was mechanically screw conducted. Anode basket made of 316 stainless steel with diameter of 10 mm and height of 30 mm was utilized. The reference electrode was a 1 wt. % Ag/AgCl electrode. Mixture of anhydrous LiCl-KCl salts with purity of 99.99% from Sigma Aldrich and anhydrous $ZrCl_4$ with purity of 99.99% from the same source was used as electrolyte. The initial concentration of $ZrCl_4$ in LiCl-KCl was 4wt.%. We could not acquire any unirradiated Zr-2.5Nb alloys same as pressure tube. So HANA cladding scrap is acquired KNF and this was used as surrogate material after conducting ICP-MS to analyze the chemical composition. The chemical composition of surrogate material is shown in Table 5.1. Zr-Nb alloy having size of about ø9.5 x 35mm were introduced into the anode basket as shown in Figure 5.1. The Zr-Nb alloy has no Ni and Co, so Ni wire and CO wire

additionally were inserted into anode basket.

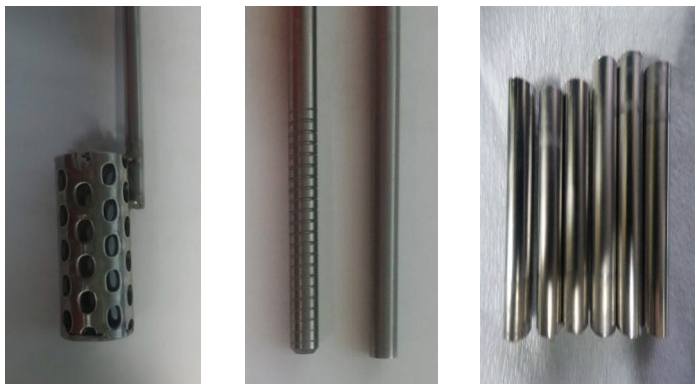

(a) (b) (c)

Figure 5.1 (a) Anode Basket (b) Cathode electrode; Left : machined, Right : no worked (c) Zr-Nb Alloys

Table 5.1 . Surrogate material Chemical composition measured by ICP-MS

Element	wt.%
Zirconium	98.093
Niobium	1.623
Impurities	0.284

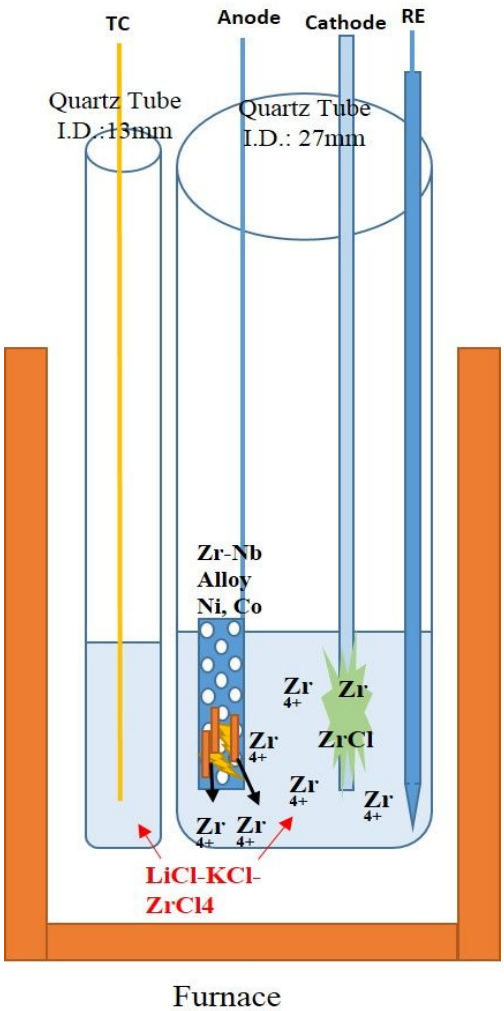

Figure 5.2 Cell and Furnace composition for Electrorefining experiment

Electrorefining main objective is to recover higher purity zirconium without impurities such as Nb, Ni, Co by suppressing dissolution of these elements. electrorefining experiments were conducted by adjusting anode or cathode potential. Since impurities have more positive apparent reduction potential than Zr as shown in Table 5.2, impurities are hard to dissolve from anode basket, however, once these are dissolved from anode, they would be deposited on cathode and contaminate cathode products. Four electrorefining experiments with 5wt.% concentrations of $ZrCl_4$ were conducted. Since open circuit voltage was about -0.9V(vs. Ag/AgCl) in the LiCl-KCl-5wt.% $ZrCl_4$ with Zr-Nb alloy as a anode, first electrorefining experiment was conducted by controlling anode potential as -0.85V(vs. Ag/AgCl) for about 38 hours. The other three experiments were conducted by controlling anode potential as -0.85V(vs. Ag/AgCl) for about 15 hours and by controlling cathode different potential as -1.0, -1.2, -1.6V(vs. Ag/AgCl) for about 5 hours. Composition of cathode deposits was investigated by Inductively coupled plasma mass spectrometry (ICP-MS) and chemical form was identified by X-ray diffraction (XRD).

Table 5.2 .Apparent reduction potential of Zr, Nb, Ni, Co on the major reaction during electrorefining of Zr-Nb alloys

[unit : V vs. Ag/AgCl]

Reaction	This work (Average)	References	Deviation for Reference
$Zr^{2+}+2e^{-}\rightarrow Zr$	-1.124	-1.266 ~ -1.007	+0.142 ~ -0.117
$Zr^{4+}+4e^{-}\rightarrow Zr$	-1.159	-1.220 ~ -1.064	+0.061 ~ -0.095
$Zr^{4+}+2e^{-}\rightarrow Zr^{2+}$	-0.906	-1.121 ~ -0.737	+0.215 ~ -0.169
$Nb^{3+}+3e^{-}\rightarrow Nb$	-0.402	-0.520 ~ -0.189	+0.118 ~ -0.213
$Ni^{2+}+2e^{-}\rightarrow Ni$	-0.065	-0.106 ~ -0.052	+0.041 ~ -0.013
$Co^{2+}+2e^{-}\rightarrow Co$	-0.270	-0.264 ~ -0.241	-0.008 ~ -0.029

Table 5.3 Applied potential and operation time condition during Electrorefining of Zr-Nb

Case	Applied Potential [V vs. Ag/AgCl]
#1	-0.85V @ Anode
#2	-0.85V @ Anode -1.00V @ Cathode
#3	-0.85V @ Anode -1.20V @ Cathode

#4	-0.85V @ Anode -1.60V @ Cathode

5.2 Electrorefining results of Zr-Nb alloys

In the #1 case experiment, cathode had no adhesive deposition as shown figure. 5.3, but black powder was recovered bottom the salts as shown figure. 5.9. According to literature studies, ZrCl is more adhesive than Zr pure metal. So this black powder was expected to be Zr metals.

Because of no deposition on the cathode for only controlling anode potential, the other experiments were additionally conducted by controlling cathode potential. As a result, there were some depositions on the cathode in shown figure 5.4, 5.5, 5.6.

All of the deposition on cathode and precipitations in salts were measured by ICP-MS and XRD. But in the #4 case experiment [-1.6V(vs. Ag/AgCl) at Cathode] deposition volume was enough not to analyze XRD and the sample of molten salts in #2 case experiment[-1.0V(vs. Ag/AgCl) at Cathode] was not applied for XRD because it could be nearly seen black powder. For #2 case experiment, soluble-soluble reaction [Zr(IV)↔Zr(II)] is major reaction. That's the reason why black powder was little. Through the ICP-MS analysis, Co was not discovered in all of the samples and Ni was discovered within background concentration of LiCl-KCl. Therefore we could conclude that Ni and Co could not be dissolved from the anode

basket. But some Nb (2.1~33.2ppm) was discovered by ICP-MS. It is very similar that Nb concentration result of Electrorefining for Zirlo by K.T. Park was under 30ppm[13]. Table 5.4 shows ICP-MS results of deposition at cathode and precipitation in the salts.

As a result of XRD analysis, it was revealed that chemical form of recovered Zr was ZrCl or ZrO_2. Since oxygen concentration in the glove box was maintained as lower than 0.1pm during electrorefining experiment, Zr was expected to be oxidized during XRD analysis.

In all of the electrorefining experiments, Zirconium purity increased from about 92% to about 99.9%. Initial Zr purity was considered including Co and Ni, so it is different from Zr purity on the Table 5.1 without Co and Ni.

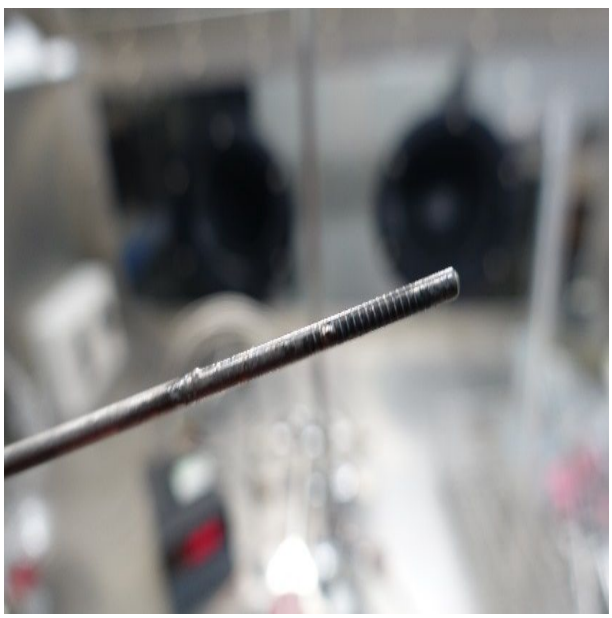

Figure 5.3 No deposition at the cathode for -0.85V of applied potential to anode potential

Figure 5.4 Deposition at the cathode for -1.0V of applied potential to cathode potential

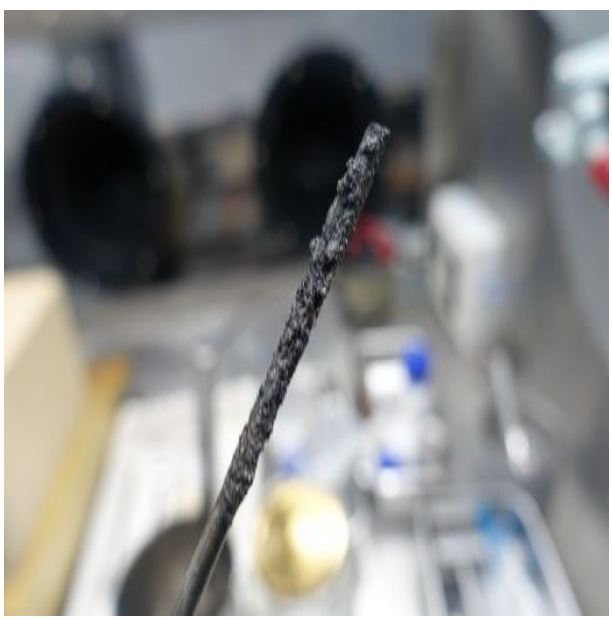

Figure 5.5 Deposition at the cathode for -1.2V of applied potential to cathode potential

Figure 5.6 Deposition at the cathode for -1.6V of applied potential to cathode potential

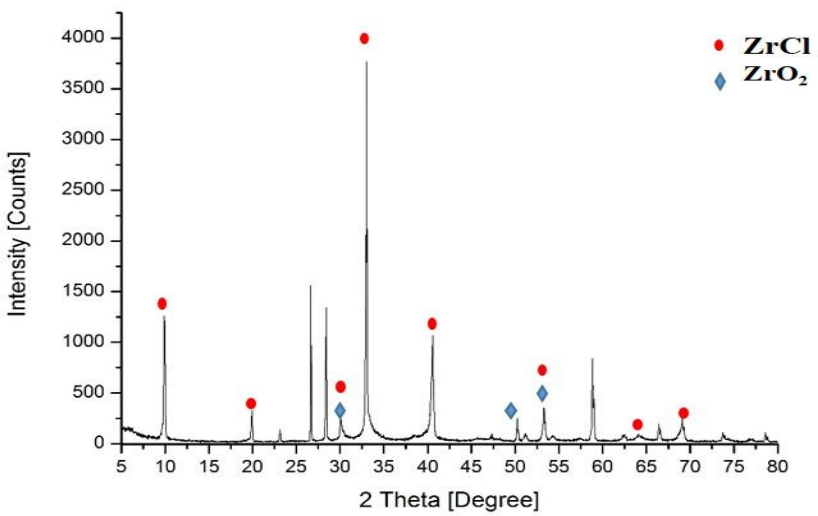

Figure 5.7 XRD Result for the Deposition at the Cathode for -1.0V of the applied potential

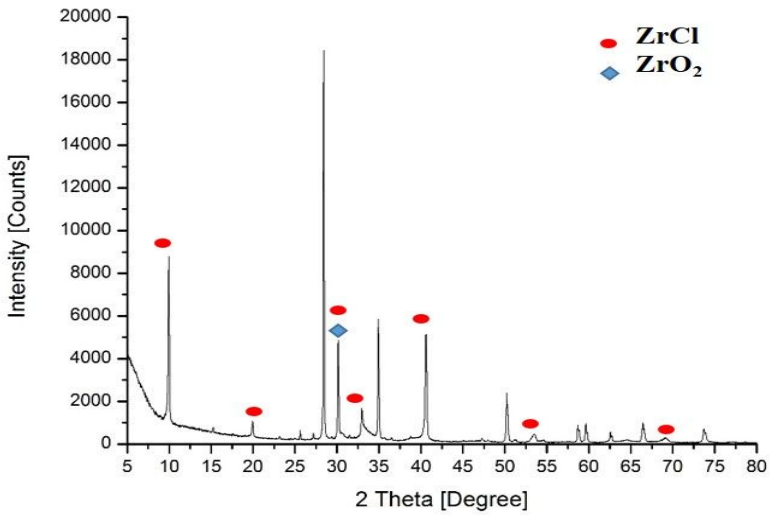

Figure 5.8 XRD Result for the Deposition at the Cathode for -1.2V of the applied potential

Figure 5.9 Molten Salts (LiCl-KCl-0.5wt% $ZrCl_4$) for -0.85V of the applied potential (Case 1) (Oxidation Experiment)

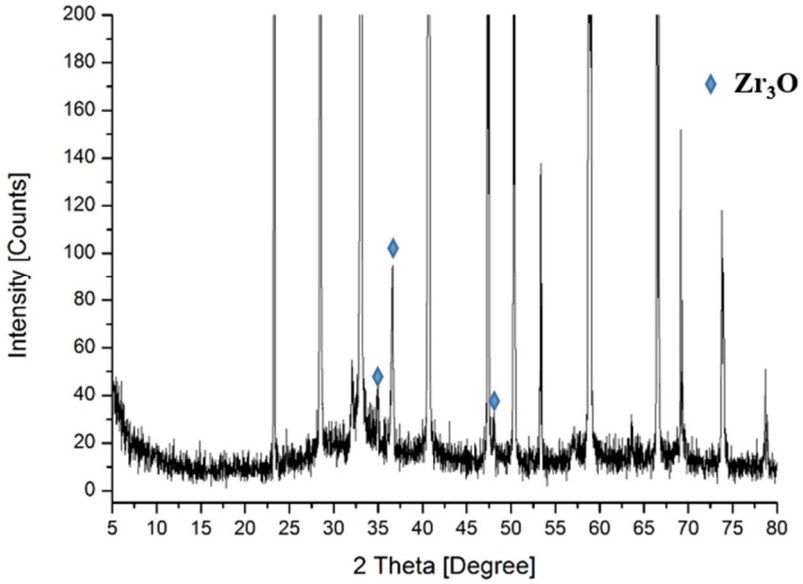

Figure 5.10 XRD result for Molten Salts (LiCl-KCl-0.5wt% $ZrCl_4$) for -0.85V of the applied potential (Case 1) (Oxidation Experiment)

Figure 5.11 Molten Salts(LiCl-KCl-5wt% $ZrCl_4$) for -0.85V and -1.0V of the applied potential (Case 2) (Oxidation + Reduction Experiment)

Figure 5.12 Molten Salts (LiCl-KCl-5wt% $ZrCl_4$) for -0.85V and -1.2V of the applied potential (Case 3) (Oxidation + Reduction Experiment)

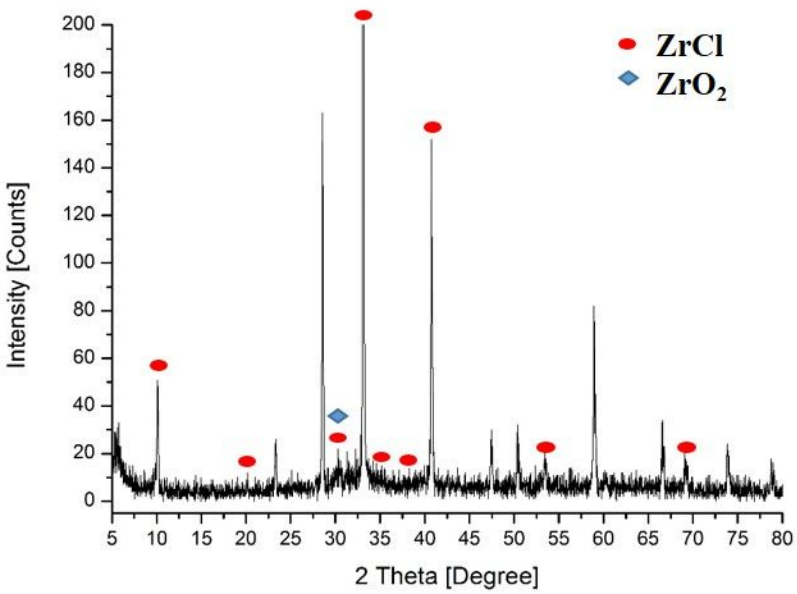

Figure 5.13 XRD result for Molten Salts (LiCl-KCl-0.5wt% $ZrCl_4$ for -0.85V and -1.2V of the applied potential (Case 3) (Oxidation + Reduction Experiment))

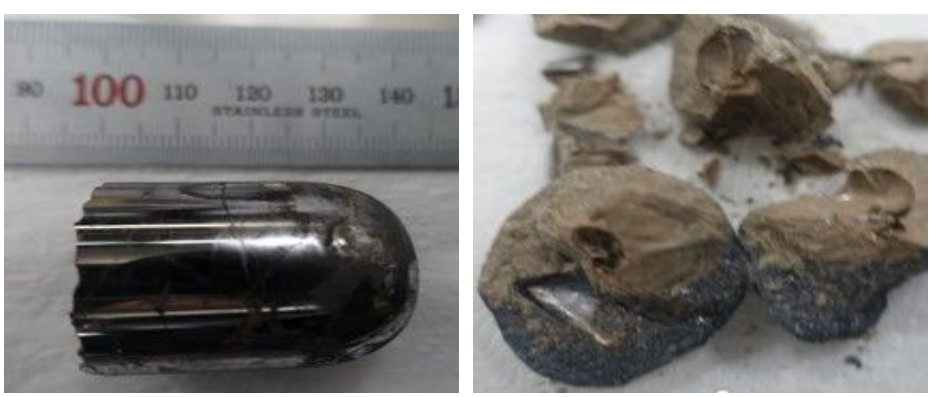

Figure 5.14 Molten Salts (LiCl-KCl-5wt% $ZrCl_4$) for -0.85V and -1.6V of the applied potential (Case 3) (Oxidation + Reduction Experiment)

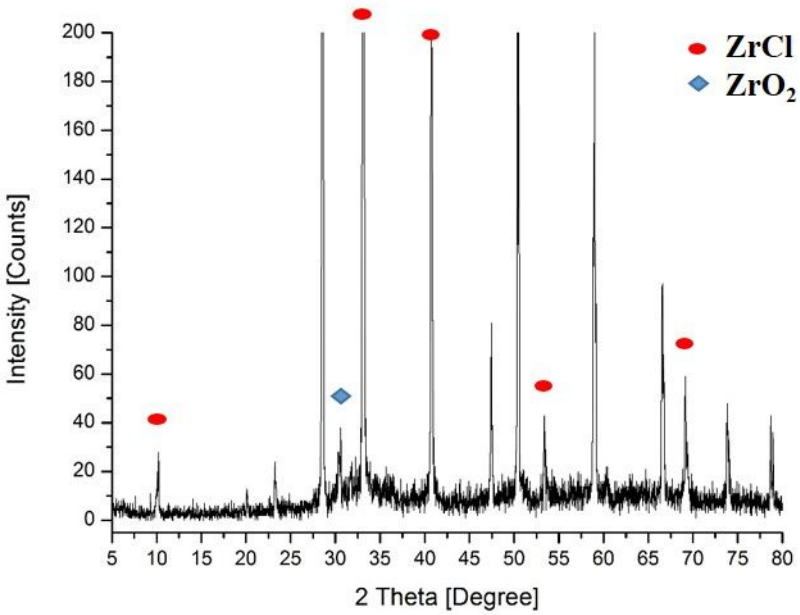

Figure 5.15 XRD result for Molten Salts (LiCl-KCl-0.5wt% $ZrCl_4$ for -0.85V and -1.6V of the applied potential (Case 4)) (Oxidation + Reduction Experiment)

During electrorefining experiments, cathode potential was different from applied potential. The difference is due to ohmic potential drop of molten salts, because molten salts play a role as impedance. As ohm's law, potential drop is proportionate to current. As shown in fig 5.16, the higher applied potential has a higher reduction current. Therefore ohimic potential drop for -1.6V is deeper than the others.

And reduction current transitions are similar to results of Zircaloy-4 electrorefining conducted by KAERI in 2012. The reduction currents begin with initial rise due to charging electric double layer and then as the diposition continues, reduction current increased due to increase of the surface area.[12]

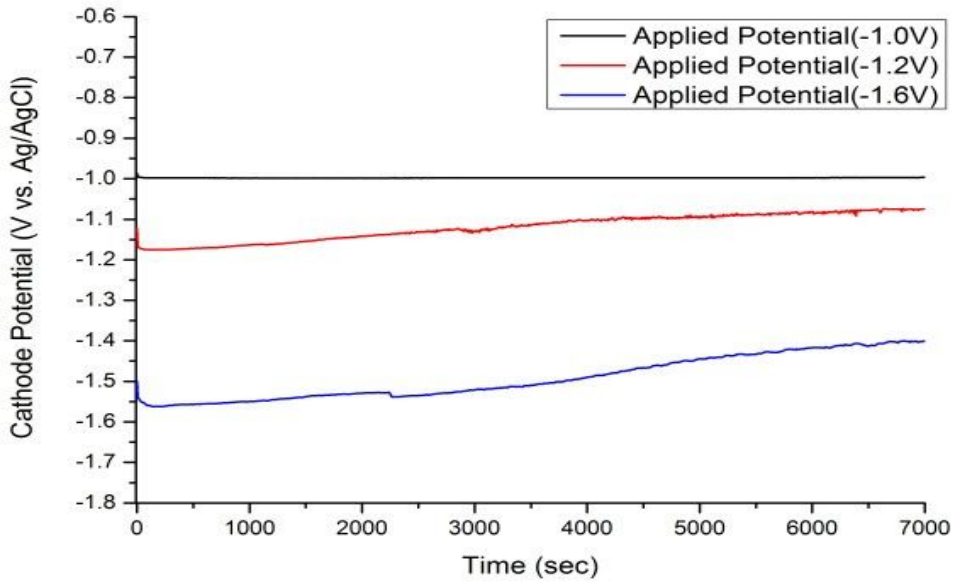

Figure 5.16 Real Cathode potential as different applied cathode potential

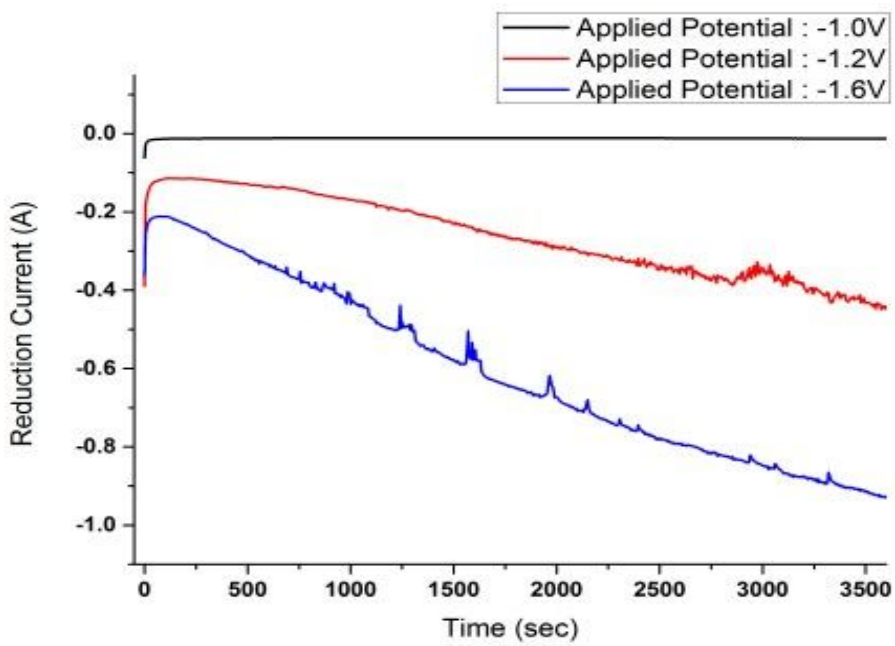

Figure 5.17 Current transients for Zr reduction at potentials of this work(-1.0V, -1.2V, -1.6V vs. Ag/AgCl in LiCl-KCl-5wt% $ZrCl_4$) at 500℃.

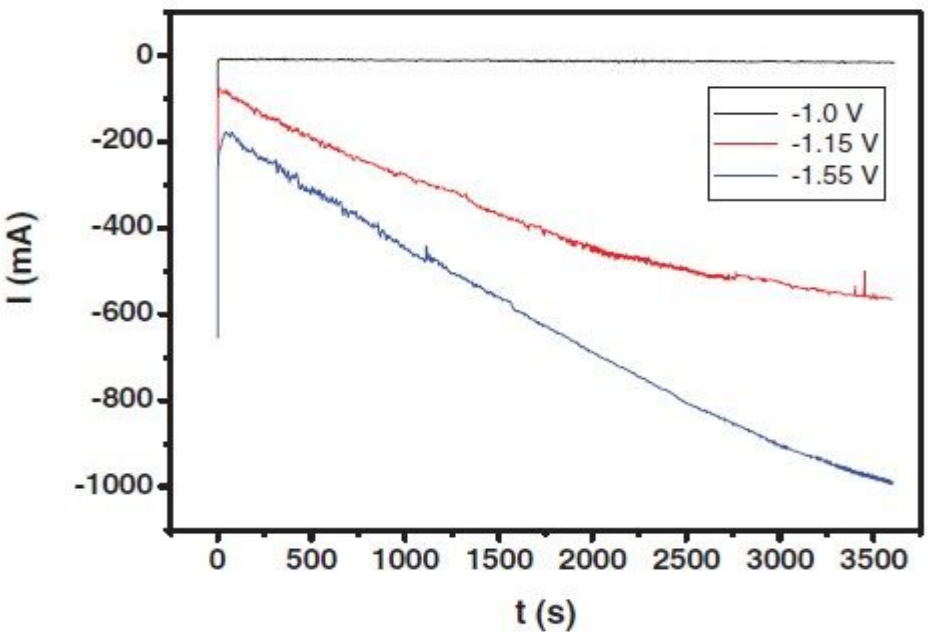

Figure 5.18 Current transients for Zr reduction at potentials of KAERI's work(2012) at 500℃[12]

Table 5.4 Concentration of Nb, Co, Ni measured by ICP-MS for #2, #3, #4 deposition at cathode(#1 : precipitation bottom molten salt)

[Unit: ppm]

Element	#1 Case	#2 Case	#3 Case	#4 Case
Nb	2.1	33.2	20.3	28.1
Co	N/D	N/D	N/D	N/D
Ni	3.82	0.4	5.6	3.2

[Background in LiCl-KCl eutectic : Nb, Co =0ppm, Ni=3.2~9.3ppm]

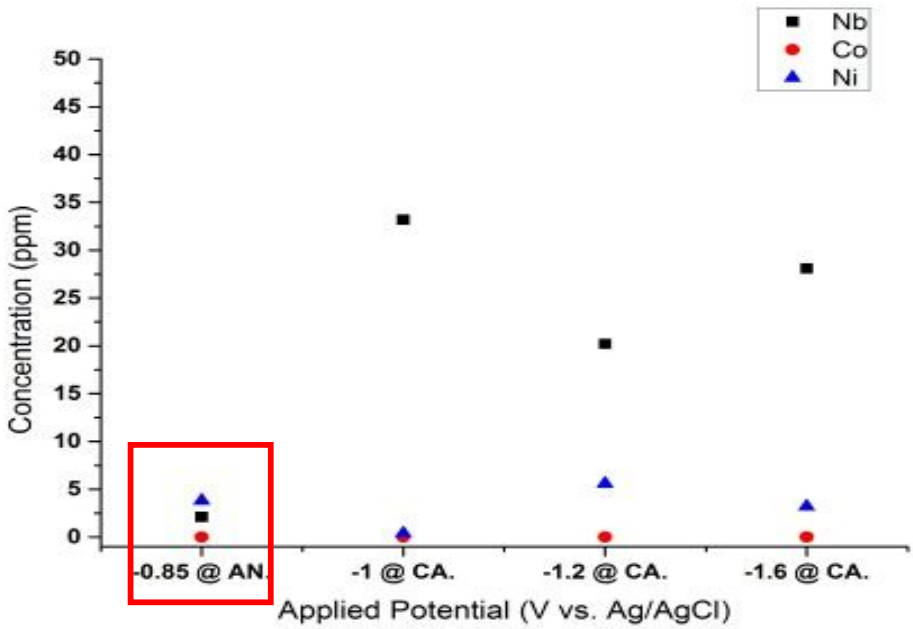

Figure 5.19 Concentration of Nb, Co, Ni measured by ICP-MS for #2, #3, #4 deposition at cathode(#1 : precipitation bottom molten salt)

5.3 Discussion

As mentioned previous chapter, Ni and Co were not discovered except backgroud concentration. This means that only one electrorefining can separate Co, Ni from Zr-Nb alloy. Literature studies for electrorefining of Zircaloy-4 showed that Co was not discovered in the deposition at the cathode.[12,16]

We thought that a few niobium were dissolved chemically rather than electrochemical reaction since it is different between Zr and Nb reduction potential. Among the four experiments, Nb concentraion[2.1ppm] of #1 case experiment was the lowest than any other experiment. Although the deposition at the cathode is none, #1 experiment condition is the best in case of seperationg Nb from Zr-Nb alloys. If it is calculated decontamination factor(DF) by using Nb concentration before (iniatial anode) and after(precipitated black powder) electrorefining experiment, DF would be about 7,100. As shown in Table 5.5, if electrorefining of irradiatied pressure tubes is conducted more than three times, intermediate level waste of them will be change to exemption waste. But we think that it should needs to compare costs between direct disposal and multi-step electrorefining.

5.3.1 Economical effect on the disposal cost

Radioactive wastes are divided into high level wastes (HLWs), Intermediate Level Wastes (ILWs), Low Level Wastes (LLWs), Very Low Level Wastes (VLLWs) as

relevant laws of Nuclear Safety and Security Commission.

Recovered Zr from electorefining of irradiated Zr alloy is radioactive. However, if recovered Zr is narrowly reused as only nuclear industry since Zr is representative metal used in nuclear power plants and is very expensive, disposal cost for radioactive wastes will be considerably reduced. According to related radioactive waste laws, disposal cost per drum of 200 liters is 12.19 million won [38].

The reduced disposal cost and the Zr recycle effect are calculated to analyze economic efficiency. To assess reduced disposal cost of domestic pressure tubes in PHWRs, it was assumed as followings. All of the pressure tubes should be replace one time, so total mass of pressure tubes is 184 tons. And recovery rate of Zr for electrorefining is 99%, packing factor of radioactive waste drums is 0.8 and waste density is similar to vitrification waste density, 2,230kg/m^3. The composition of pressure tube for PHWRs is equal to ASTM B353-12, Zr-2.5Nb. Zr weight percent (wt.%) is 96.93955 in Zr-2.5Nb. Reduced disposal cost is calculated by following relation.

Reduced disposal cost [₩]

= Total disposal cost of radioactive wastes – waste disposal cost except Zr

= disposal cost of recovered Zr

= Total waste mass[kg] ÷ waste density[kg/m^3] ÷ volume of a drum [m^3/drum] ÷ packing factor × disposal cost per drum[₩/drum] × (recovery rate of Zr × mass fraction of Zr)

= 184E3[kg]÷2230[kg/m^3]÷0.2[m^3/drum]÷ 0.8 ×1.219E7[₩/drum] ×

(0.9693955×0.99) = ₩ 6 billion

5.3.2 Radioactive wastes volume reduction effect

As the 5.3.1 chapter mentioned, recovered Zr will have effect for wastes volume reduction as well as economical effect. Volume reduction is equal to recycled Zr volume. All assumptions are equal to previous chapter. Volume reduction relation is as follows.

Reduced drums = volume of recovered Zr

; Total waste mass[kg] ÷ waste density[kg/m^3] ÷ volume of a drum

[m^3/drum] ÷ packing factor × (recovery rate of Zr × mass fraction of Zr)

In calculating as above the relation, the number of volume reduction drums is about 500 drums. That is, 500 waste drums will be reduced through the electrorefining of pressure tubes in PHWRs of KOREA. It can be thought that reduction volume is a few, but if HANA cladding made from Zr-Nb alloy is commercialized, volume reduction effect will be enormous. And reduction of radioactive wastes is considered that it is essential to operate disposal repository effectively and public acceptance for nuclear power plant may highly increase.

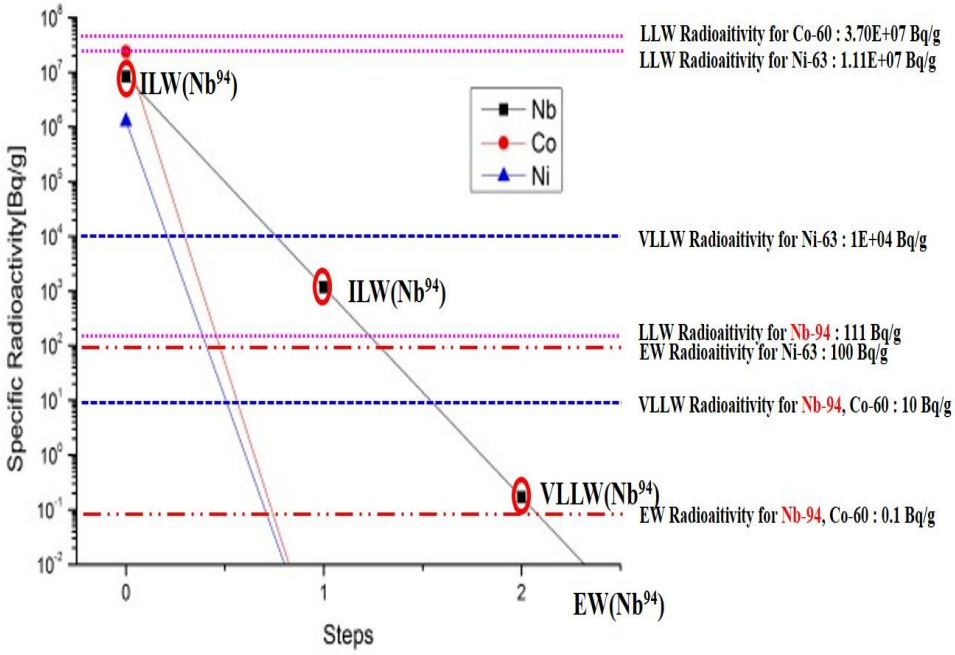

Figure 5.20 As Electrorefining step of irradiated pressure-tube (Zr-2.5Nb), radioactive level change for Nb^{94}, Co^{60}, Ni^{63}.

Table 5.5 Radioactive waste level of Nb^{94}, Co^{60}, Ni^{63} as Electrorefining steps

Element	Step 0	Step 1	Step 2	Step 3
Nb-94	ILW	ILW	VLLW	EW
Co-60	LLW	EW	EW	EW
Ni-63	LLW	EW	EW	EW

[ILW : Intermediate Level Waste, LLW : Low Level Waste, VLLW : Very Low Level Waste, EW : Exemption Waste]

5.4 Computational analysis of the electrorefining

After the electrorefining experiment, 1-D Computational simulation was conducted for same electrerefining conditions. The used computational code was REFIN named 1-D time-dependent code for electrochemical reactions. In REFIN, to utilize modified Butler-Volmer equation, it assumed that all the electrochemical reaction are one-step reaction [39]. So REFIN code can't reflect disproportionation of Zr or Nb. For electrochemical reaction of Zr and Nb, it was only considered $Zr(IV) + 4e^- \rightarrow Zr$ and $Nb(III) + 3e^- \rightarrow Nb$ and other reaction were ignored. Current input was used average real reduction current in the several ranges because current was changed during experiment. Anode mass for input file was equal to real experiment condition. We would like to check composition of deposition at the cathode, REFIN simulation result should be compared to the #2, #3, #4 case experiment since there was no deposition at the cathode in the #1 case experiment. Therefore it assumed that initial molten salt composition was equal to black powder in the #1 case experiment.

#2, 3, 4 case experiment conducted applying potential at the cathode for 5 hours. REFIN results at 5 hours were compare to experiment results as shown in Table 5.6. We could check that each result was very similar.

As shown in Figure 5.20, Zr is expected to dissolve the fastest among Zr, Nb, Co, Ni in LiCl-KCl at 500°C, because Zr is the most oxidizing element in these

elements. The order of reduction at cathode is reverse to oxidizing as shown in figure 5.21.

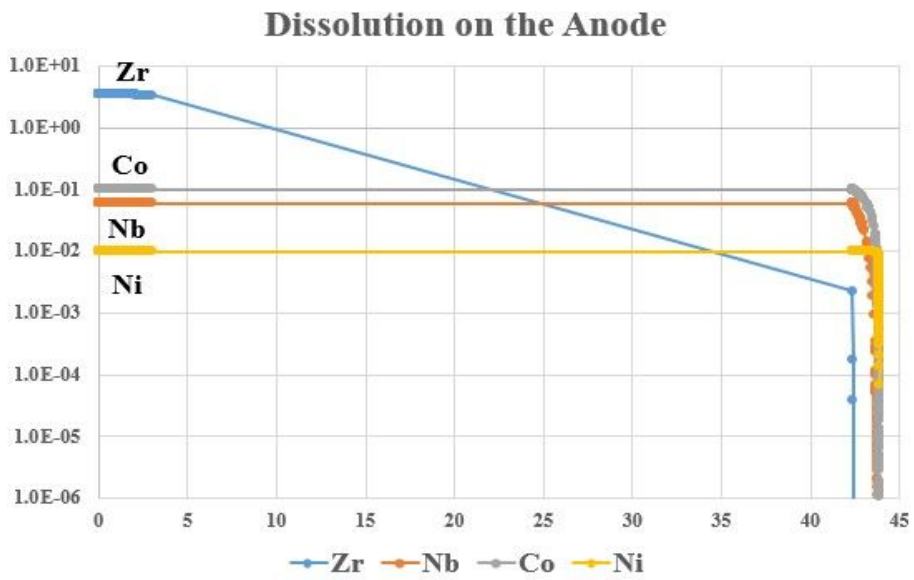

Fig 5.21 Dissolution behavior on anode during electrorefining simulated by REFIN

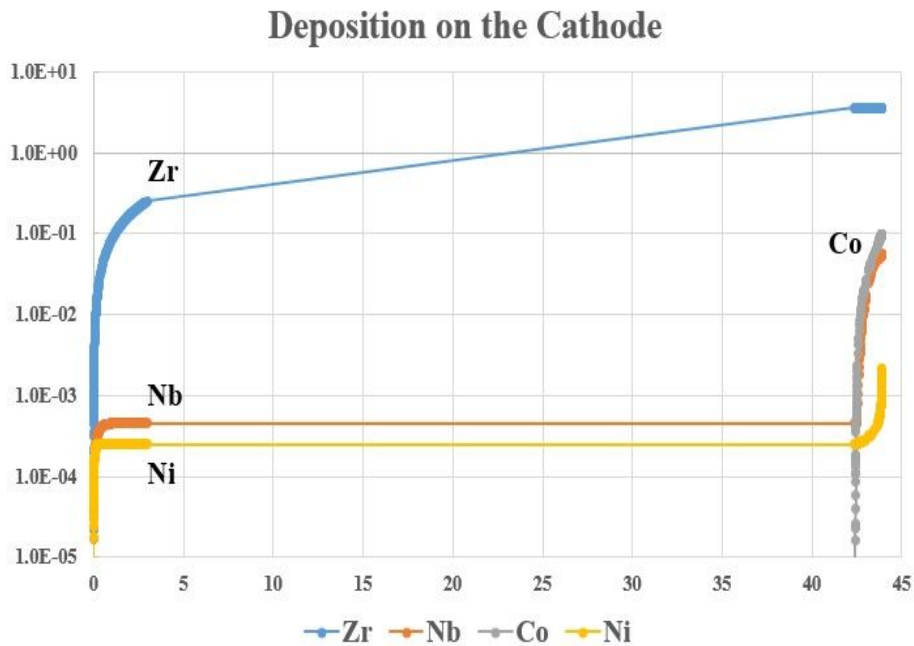

Fig 5.22 Deposition behavior on cathode during electrorefining simulated by REFIN

Table 5.6 The composition of deposition at the cathode (*N/D<0.002ppm)

Element	Experimental Results [wt.%, Average]	Computational Simulation by REFIN[wt.%]
Zr	99.90 [99.63~99.98]	99.83
Nb	0.09 [0.02~0.15]	0.11
Co	*N/D	0
Ni	0.01 [0.01~0.02]	0.06

6. Conclusions and Future Work

6.1 Conclusions

The main goal of this thesis is develop methods for disposing of pressure tubes (Zr-2.5Nb) wastes of PHWR in the LILW repository. Mass of disposable irradiated pressure tubes is almost nothing. The reason is why the expected specific radioactivity of Nb^{94} for pressure tubes is very high and the half -life of Nb^{94} is very longer than the other nuclides. If Nb^{94} is removed from irradiated pressure tube wastes, they can be disposable in the LILW repository. Partitioning impurities such as Nb, Ni, Co was checked by conducting electrochemical experiments and was verified by computational 1-D analysis, REFIN.

The elecrorefining, one of pyroprocessing technologies, uses the redox potential difference among the elements. First of all, Nb, Co and Ni are determined to remove from irradiated pressure tubes by computational analysis ORIGEN2.

Zr, Nb, Co, Ni redox mechanism was determined through the cyclic voltammetry experiments. Zr cyclic voltammetry experiments were conducted in 2wt.%, 1wt.%, 0.5wt.%, 0.2wt.% ZrCl4-LiCl-KCl, respectively. Zr redox mechanism features disproportionate reactions. In the low concentration (0.2wt.%, 0.5wt.%), major soluble-insoluble reaction was showed $Zr^{4+} + 3e^{-} \leftrightarrow ZrCl$. But in high concentration(1wt.%, 2wt.%), soluble-insoluble reaction also was show Zr^{+} +

$e^- \leftrightarrow Zr$ as well as $Zr^{4+} + 3e^- \leftrightarrow ZrCl$. ZrCl is more adhesive than pure Zr metal, so the deposition at cathode electrod was mainly ZrCl and few Zr. Nb redox mechanism is more complicated than Zr redox mechanism. Nb redox mechanism has disproportionate reaction and nonstoichiometric reaction. Nb made subchloride in chloride salt below 650°C. Nb_3Cl_8 is major Nb subchloride. Major reductive reaction is $Nb^{3+} + 3e^- \leftrightarrow Nb$ and if Nb_3Cl_8 is in molten salts, other two reduction steps will be generated such as $Nb^{3+} + e^- \leftrightarrow Nb^{2+}$ and $Nb^{2+} + 2e^- \leftrightarrow Nb$. Ni and Co redox mechanism are very simple as one-step reduction. Ni redox mechanism is $Ni^{2+} + 2e^- \leftrightarrow Ni$ and Co redox mechanism is $Co^{2+} + 2e^- \leftrightarrow Co$.

As conducted cyclic voltammetry experiments, Zr is the most oxidative among the elements. To dissolve only Zr, anode potential was controlled by Zr oxidation potential (-0.85V vs. Ag/AgCl). During electrorefining, applied potential at the anode was constant for 38 hours. There was no deposition at the cathode electrode and some black powders were at the bottom of the salts. To make depositions at the cathode, working electrode was changed from anode to cathode and applied potential at the cathode (-1.0, -1.2, -1.6V vs. Ag/AgCl) was constant for about 5 hours. Depositions at the cathode were analyzed by ICP-MS and XRD. As results of ICP-MS, Co was not discovered in all samples and Ni was only discovered within background concentration of LiCl-KCl. Thus, it was thought that Co and Ni were not dissolved from anode. Some Nb was discovered under the 30 ppm. It was thought that Nb was not dissolved electrochemically, but chemically.

Since electro-reduction potential difference between Zr and Nb is about 0.4V. For electrorefining of applied anode potential (-0.85V vs. Ag/AgCl), Nb concentration of 2.1 ppm was the lowest in all cases. Decontamination factor was assessed about 7,100 by using this result. Consequently, decontamination processes of electrorefining for irradiated pressure tube to be needed to change from ILW to EW are three times. If recovered Zr through electrorefining is narrowly recycled to nuclear industry, economical effect will be about 19 billion won and the volume reduction drums is about 500 drums.

Electrochemical decontamination such as electrorefining is not yet commercialized, but it is effective to remove a certain radionuclide in case of big difference among elements. We can suggest that surface decontamination such as dry or wet type is the first conducted to lower radioactivity and next, melting decontamination is used to remove a volatile radionuclide and to make representative sample. Finally, electrochemical decontamination should be used to separate a certain radionuclide such as Nb^{94} has a long half-life and high radioactivity from irradiated pressure tubes. If recovered Zr is recycled and the other radionuclide undergo transmutations or is dispose of in the high level waste disposal repository, disposal problem for irradiated pressure tubes will be solved.

6.2 Future work

This dissertation shows that Co and Ni were fully separated from Zr-Nb alloy, but some Nb was recovered with Zr and ZrCl. Since it needs to fully separate Nb from Zr-Nb alloy, additional experiments should be conducted as follows.

1. Various applied potential at the anode or the cathode

    - An optimized applied-potential should be searched for no Nb deposition through additional experiments.

2. Using LiF-KF molten salts instead of LiCl-KCl

    - Disproportionate reaction of Zr does not appear in fluorine salts.

3. Higher experimental temperature than 650°C

    - In a higher temperature than 650°C, Nb does not make a subchloride .

If additional experiment is conducted as above conditions, it is expected that Nb may be fully separated from Zr-Nb alloy.

Bibliography

[1] IAEA Power Reactor Information System (2016, June, 15th), Operational Reactors by Age, World Statistics. Available: https://www.iaea.org/PRIS/WorldStatistics/OperationalByAge.aspx.

[2] KHNP, 2012, Nuclear Power Whitepaper.

[3] KORAD, Construction Project, Available: http://www.korad.or.kr/krmc2011/eng/construction/ke04_01.jsp.

[4] KHNP, 2014, Feasibility Study on Treatment and Recycling for Radioactive Metal Waste, Technical Report, 2014-50003339-단-0407TR PF01086.

[5] G.P. Sabol, G.D. Moan, 2000. Zirconium in the Nuclear Industry: Twelfth International Symposium, ASTM International.

[6] E.D. Collins, G.D. DelCul, B.B. Spencer, R.R. Brunson, J.A. Johnson, D. Terekhov, N.Emmanuel, 2012. Process Development Studies for Zirconium Recovery/Recycle from used Nuclear Fuel Cladding. Procedia Chemistry 7, 72-76.

[7] H.G. Kim., J.Y. Park, Y.H. Jeong, Y.H. Koo, J.S. Yoo, Y.K. Mok, Y.H Kim, J.M. Suh, 2014, In-Pile Performance of HANA cladding tested in HALDEN Reactror, Nuclear Engineering and Technology, vol.46, No.3.

[8] WIKIPEDIA, Zirconium alloy, Available: https://en.wikipedia.org/wiki/Zirconium_alloy.

[9] ASTM B353-12, 2013, Standard Specification for Wrought Zirconium and Zirconium Alloy Seamless and Welded Tubes for Nuclear Service (Except Nuclear Fuel Cladding).

[10] Canadian Nuclear Safety Commission (CNSC), 2003, Reactor Physics, rev.1, page 90.

[11] KORAD, 2008, Safety Analysis Report, rev.1, Chapter 8.2.2.

[12] C.H. Lee, K.H. Kang, M.K. Jeon, C.M. Heo, Y.L. Lee, 2012, Electrorefining of Zirconium from Zircaloy-4 Cladding Hulls in LiCl-KCl Molten Salts, Journal of the Electrochemical Society, Vol.158, pages 463-468.

[13] K.T. Park, T.H. Lee, N.C. Jo, H.H Nersisyan, B.S.Chun, H.H.Lee, J.H.Lee, 2013, Purification of nuclear grade Zr scrap as the high purity dense Zr deposits from Zirlo scrap by electrorefining in LiF–KF–ZrF4 molten fluorides, Journal of Nuclear Materials, Vol.436, pages D130-D138.

[14] K. Laing, J. Hampshire, D. Teer, G. Chester,1999, The effect of ion current density on the adhesion and structure of coatings deposited by magnetron sputter ion plating, Surface coating Technology. Vol.112, pages 177-180.

[15] R.Fujita, H.Nakamura, Y.Haruguchi, R.Takahashi, M.Sato, T.Shibano, Y.Ito, T.Goto, T.Terai, S.Ogawa, 2005, Development of Zirconium Recovery Process for Zircaloy Cladding and Cannel Boxes from Boiling Water Reactors by Electrorefining in Molten Salts, Proceedings of ICAPP '05, paper 5686.

[16] J.Y. Park, 2014, Electrorefining of Irradiated Spent Nuclear Fuel Zircaloy-4 Cladding in LiCl-KCl Molten Salts, Doctoral Dissertation.

[17] WIKIPEDIA, Cyclic Voltammetry, Available: https://en.wikipedia.org/wiki/Cyclic_voltammetry

[18] A.J. Bard, 1976, Encyclopedia of Electrochemistry of the Elements, Vol. X, Fused Salt Systems, Marcel Dekker, Inc., New York.

[19] S.A. Kuznetsov, H. Hayashi, K. Minato, and M. Gaune-Escard, 2005, Electrochemical Behavior and Some Thermodynamic Properties of UCl4 and UCl3 Dissolved in a LiCl-KCl Eutectic Melt, Journal of the Electrochemical Society, 152(4), C203-C212.

[20] P. Masset, D. Bottomley, R. Konings, R. Malmbeck, A. Rodrigues, J. Serp, and J.Glatz, 2005, Electrochemistry of Uranium in Molten LiCl-KCl Eutectic, Journal of the Electrochemical Society, 152(6), A1109-A1115.

[21] R.O. Hoover, 2014, Uranium and Zirconium Electrochemical Studies in LiCl-KCl Eutectic for fundamental Applications in Used Nuclear Fuel Reprocessing, Doctoral Dissertation.

[22] J.M. Ko, 2012, Cyclic Voltammetry for the Polymers, Polymer Science and Technology Vol.23, No.6.

[23] A.J. Bard and L.R. Faulkner, 2001, Electrochemical Methods: Fundamentals and Applications Second Edition, John Wiley & Sons, Inc., New Jersey.

[24] S. Ghosh, S. Vandarkuzhali, P. Venkatesh, G. Seenivasan, T. Subramanian, B.

Prabhakara Reddy, K, Nagarajan, 2009. Electrochemical studies on the redox behaviour of zirconium in molten LiCl–KCl eutectic. Journal of Electroanalytical Chemistry, Vol. 627, pages 15-27.

[25] Y. Sakamura, 2004. Zirconium behavior in molten LiCl-KCl eutectic. Journal of The Electrochemical Society, Vol.151, pages C187-C193.

[26] R.Baboian, D.L. Hill, R.A. Bailey, 1965, Electrochemical Studies on Zirconium and Hafnium in Molten LiCI-KCI Eutectic, Journal of the Electrochemical Society, Vol.112, No.12, page 1222.

[27] CRIEPI, 1994, Pyrometallurgy Data Book, Report T93003.

[28] J.A. Plambeck, 1967, Electromotive Force Series in Molten Salts, Journal of Chemical and Engineering Data, Vol.112, No.1.

[29] M. Simpson, I.S. Hwang, 2014, Investigation of Electrochemical Recovery of Zirconium from Spent Nuclear Fuels, INL, INL/EXT-14-32065.

[30] F. Lantelme, A. Barhoun, J. Chevalet, 1993, Electrochemical Behavior of Solutions of Niobium Chlorides in Fused Alkali Chlorides, Journal of Electrochemical Society, Vol.140, No.2.

[31] M. Mohamedi, Y. Sato, T. Yamamura, 1999, Examination of niobium electrochemistry from the reduction of Nb_3Cl_8 in molten LiCl-KCl eutectic, Electrochimica Acta, Vol. 44. Pages 1559-1565

[32] F. Lantelme, Y. Berghoute, A. Salmi, 1994, Cyclic voltammetry at a metamc electrode: application to the reduction of nickel, tantalum and niobium salts in fused electrolytes, Journal of Applied Electrochemistry, Vol. 24, pages 361-367

[33] F. Lantelme, H.Groult, 2010, Niobium and titanium electrowinning in fused Salts, Mineral processing and Extractive Metallurgy, Vol.19, No.2.

[34] W.K. Behl, 1971, Linear Sweep Voltammetry of Ni(ll), Co(ll), Cd(ll), and Pb(ll) at Glassy Carbon Electrodes in Molten Lithium Chloride-Potassium Chloride Eutectic, Journal of the Electrochemical Society, Vol.118, No.6.

[35] K.E. Johnson, J.R. Kickinson, 1973, High-temperature Coordination chemistry of Group III, Advances in molten salts chemistry, Vol.2, Chap.3.

[36] H.A. Laitinen, C.H. Liv, 1958, An Electromotive Force Series in Molten Lithium Chloride-Potassium Chloride Eutectic, Journal of the American Chemical

Society, Vol.80.

[37] H.A. Laitinen, H.C. Gaur, 1958, Chronopotentiometry in Fused Lithium Chloride-Pottassium Chloride, Analytica Chimica Acta, Vol. 18.

[38] Ministry of Trade, Industry and Energy, ACT No. 2015-132, Rule for estimating standard of Radioactive Wastes and Used Nuclear Fuel management cost.

[39] B.G. Park, I.S. Hwang, 1999, Simulation of Electrorefining Process Using Time-dependent Multi-component Electrochemical Model: REFIN, Proceeding of the Korean Nuclear Society Autumn Meeting.

국문 요약서

전세계적으로 445기의 원자력 발전소가 운전을 하고 있으며 워자력 발전소의 운전이력 분포를 보면 30년 이상의 노후 발전소의 비중이 크다. 국내의 경우 고리1호기와 월성1호기는 설계수명(30년)을 초과하여 계속운전을 하고 있으며, 계속운전을 위해서는 원자력발전소의 노후설비 교체가 필수적이다. 예를 들어, 월성1호기는 원자로의 핵심설비인 압력관 전량 교체하였다. 교체된 설비는 발전소내 방사성폐기물 저장시설에서 보관되고 있다. 그리고 고리1호기는 2017년 6월, 계속운전이 끝나면 영구정지되어 관련 법령 및 규정에 따라 규제기관에 해체계획서를 제출하여 승인 받은 후 해체될 예정이다. 1단계 중저준위 방사성 폐기물 처분장이 건설되어 2015년부터 운영되고 있지만, 운영원전과 해체원전에서 발생하는 방사성폐기물로 인해 2055년 이후 처분장이 포화될 것이라는 한국수력원자력의 연구결과가 있다. 따라서 처분장의 효율적인 운영과 처분비용 절감을 위해 방사성폐기물을 줄이기 위한 제염기술 개발이 계속되어야 하는 상황이다.

원자력발전소에서 사용되는 금속 중, Zr은 고가금속이지만 열중성자 흡수단면적이 작으며, 기계적 성질이 우수하여 원자력발전소에서 많은 분야에서 사용된다. Zr에 Nb을 첨가하면 특히 내부식성이 향상되므로, Zr-Nb계열 합금은 가압경수로와 중수로에서 구조재, 피복관, 압력관으로 사용되고 있다. 또한, KAERI에서는 기존 핵연료의 지르칼로이-4 피복관에 Nb을 첨가하여 HANA피복관을 개발하였고 연구로와 상업용 원자로에 설치하여 실증시험을 거쳤다. HANA 피복관이 상용화 된다면 ZR-Nb 합금의 방사성폐기물이 급격하게 증가될 것으로 예상된다.

ORIGEN-2를 이용하여 중수로 원자로 압력관(Zr-2.5Nb)이 30년 동안 운전된 경우를 가정하여 모델링 한 결과, 냉각기간 10년이 지났을 경우

Nb^{94}, Co^{60}, Fe^{55}, Ni^{63} 순서대로 비방사능이 높은 것으로 평가되었고, 특히 Nb^{94}은 반감기가 20,300년으로 다른 핵종에 비해 매우 길기 때문에 방사화된 Zr-Nb합금에서 문제가 된다. 방사화된 중수로 압력관은 중준위 폐기물로 평가되며 관련 고시에 따라 동굴처분 되어야 한다. 1단계 중저준위처분장의 안전성분석보고서 8.2장에 따르면 Nb^{94}의 처분가능한 총 방사능량이 8.59×10^{10}Bq이다. 이 값을 근거로 처분가능한 압력관의 질량을 계산하였을 때 약 10kg만 처분가능한 결과가 나온다. 월성1호기에 교체된 압력관의 질량이 약 23톤인 것을 고려하면 처분가능한 압력관이 거의 없는 것으로 평가된다. 그리고 현재 한국원자력환경공단의 방사성 폐기물 인수기준은 저준위폐기물 기준을 따르고 있어서 저준위폐기물만 반입가능한 상태이다. 폐기물 인수기준이 바뀌기 전에는 인수기준을 만족하기 위해 중준위 방사성 폐기물을 저준위 방사성 폐기물로 낮춰야 처분이 가능하다. 방사화된 압력관에서 제염을 통해 Nb^{94}을 제거한다면, 나머지 핵종들 기준으로는 처분이 가능한 것으로 평가되었다. 따라서 본 논문에서는 핵종들 사이의 환원전위차를 이용한 전해정련을 통해 Zr-Nb합금에서 Zr과 Nb의 분리하고, 자체처분을 위해서 필요한 전해정련 단계를 평가하는 것을 목표로 한다.

피복관의 주요 재료인 지르칼로이 및 Zirlo의 전해정련에 대한 선행연구가 몇 차례 수행되었으며, Zr을 음극에 회수하여 Zr의 순도가 증가하고 불순물의 함량은 낮아진 결과가 나왔다. 이러한 선행연구를 통해 전해정련을 이용하면 방사성폐기물에서 불순물로서 Nb의 함량을 낮출 수 있을 것으로 예상된다. 선행연구에서 사용된 용융염은 불화물(LiF-KF) 또는 염화물(LiCl-KCl)이 주로 사용되었다. 불화물 계열 용융염은 순도가 높은 Zr을 얻을 수 있고 산화환원이 1단계로 나타나는 장점이 있으나, 녹는점이 높아 전해정련 운전온도가 높고, 재료의 부식을

일으키는 단점이 있다. 염화물 계열은 전해정련 운전온도가 낮고 부식문제가 불화물에 비해 적으나, 염화물 내에서 Zr이 산화환원 거동이 매우 불안정하여 '*Zr(IV) + Zr ↔ 2Zr(II)*'과 같은 불균등반응이 일어나고, ZrCl이 형성되어 전착되는 문제가 있다. 본 논문에서는 실험실 규모에서의 실험을 위해 운전온도가 상대적으로 낮고 구조재의 부식문제가 적은 염화물을 용융염으로 실험을 수행하였다.

압력관 방사성 폐기물내 핵종의 비방사능과 반감기를 고려하여 폐기물로부터 분리하고자 하는 방사성 핵종을 Nb, Co, Ni로 선정하였다. 전해정련을 위한 각 원소들의 산화환원 거동을 알아보기 위해 Zr, Nb, Co, Ni 원소들의 염화물을 LiCl-KCl 용융염에 녹인 후 500℃에서 순환전압법을 실험을 수행하여, 선행연구 결과와 비교하여 각 피크에 대한 산화환원 거동을 확인하였다.

Zr은 3개의 환원피크가 나타났으며, 용융염 내의 ZrCl4의 농도가 낮은 경우(0.2wt%, 0.5wt%)는 Zr(IV)이 ZrCl로 환원되는 속도가 ZrCl에서 Zr금속으로 환원되는 속도보다 느리므로 -1.5V(vs. Ag/AgCl)부근에서 나타나는 $ZrCl + e^- \rightarrow Zr$ 환원피크가 나타나지 않았다. 따라서 상대적으로 $ZrCl_4$ 낮은 농도에서는 ZrCl 형성이 억제되어 음극에 전착될 가능성이 낮을 것으로 보이므로 염화물 용융염 사용 시 ZrCl 전착 문제를 해결 할 수 있을 것으로 예상된다. Zr 순환전압법 결과, -1.0[V vs. Ag/AgCl] 부근에서 *Zr(IV)↔Zr(II)* 환원피크가 나타났으며, -1.2[V vs. Ag/AgCl] 부근에서 *Zr(IV)↔ZrCl* 환원피크가 나타났다. 산화피크는 -0.9 ~ -0.7[V vs. Ag/AgCl] 부근에서 일어났다.

Nb도 LiCl-KCl 용융염에서 Zr과 같이 이온간의 불균등반응이 일어나 산화환원 거동이 매우 복잡하게 나타난다. 특히 $NbCl_y$에서 y=2.33 ~ 3.13의 범위로 나타나며 비화학양론적 반응이 나타난다. 주로 형성되는 차염화물(subchloride)은 Nb_3Cl_8이다. Co와 Ni은 Zr과 Nb과 달리 이온이

바로 금속으로 환원되는 단일 산화환원 거동을 보였다.

Zr, Nb, Co, Ni의 순환전압법 결과 Zr이 가장 산화경향성이 컸으며, Zr의 산화전위에 맞춰 LiCl-KCl-5wt% $ZrCl_4$ 용융염을 사용하여 실험실 규모의 비방사화 Zr-Nb 합금의 정전압 전해정련 실험을 수행하였다. Zr-Nb 합금의 ICP-MS 분석결과 Co, Ni이 포함되어 있지 않아 양극에 Co, Ni을 추가로 삽입하여 실험을 수행하였다. -0.85[V vs. Ag/AgCl]에서 정전압 전해정련 실험을 하였으나, 음극에는 전착물이 생기지 않고 분말형태로 용융염 바닥에 가라앉았다. 따라서 일정시간 동안 산화전위를 양극에 인가하여 용해시킨 후, 작업전극을 음극으로 바꿔서 Zr환원 전위(-1.0~-1.6[V vs. Ag/AgCl])로 환원실험을 수행하였다. 환원실험 결과 음극에 전착물이 생성이 되었고 해당 전착물은 ICP-MS와 XRD를 통해 성분 및 화합물 형태를 분석을 하였다. 분석 결과 실험조건의 용융염(5wt%)의 ZrCl4의 농도가 순환전압법에서 사용한 농도(0.1~2wt%) 보다 높은 편이라 ZrCl형태로 전착이 된 것을 확인 할 수 있었으며, 부분적으로 ZrO_2형태로 전착된 것이 확인 되었다. 글로브박스 내부 산소 농도는 0.1ppm이하로 유지하고 있었으므로, XRD 분석시 Zr 금속이 산화된 것으로 예상된다. 전해정련 전후 양극과 음극의 Zr 순도 비교 시 모든 실험조건에서 순도가 91~93%에서 99%이상으로 증가하였다. Nb은 음극 전착물에서 극소량 측정이 되었는데, 이것은 환원실험에서 상대전극 이었던 양극에서 소량 화학적으로 용해되어 용융염이 음극에 Zr과 공전착될 때 포함된 것으로 예상된다. Co는 모든 경우에서 검출되지 않았으며, Ni은 용융염 내의 포함되어 있던 불순물 농도 이내로 검출되어 Zr-Nb의 전해정련으로는 용해되지 않은 것으로 평가된다.

전해정련 전후 불순물들의 농도로 제염계수를 평가하였고, 냉각기간 10년의 압력관 방사성폐기물을 자체처분 할 시 필요한 전해정련 단계는 실험결과 3단계가 필요한 것으로 평가되었다. 방사화된 폐기물에서

회수된 지르코늄은 Zr-93의 방사성핵종이 포함되어 있으므로 일반 산업용이 아닌 원전방사성폐기물 저장용 드럼 등 원자력산업에 재활용할 수 있을 것이다. 국내 중수로 4기에 대해 압력관 1회 교체를 가정한 Zr 재활용효과는 경주 처분장 폐기물을 약 500드럼 절감할 것으로 평가되고, 또한 경제적 효과는 약 190억원의 절감효과가 있는 것으로 평가되었다.

전해정련을 통해 분리되어 재활용되지 못한 소량의 방사성 폐기물(Nb-94, Co-60, Ni-63등)은 현재 개발중인 4세대 고속로 또는 가속기를 통해 저방사능, 단반감기 핵종으로 핵변환시키거나 고준위 방사성폐기물 처분장에 처분한다면 방사성폐기물 처분문제를 해결 할 수 있을 것이다. 기존 표면제염 및 용융제염을 통해서는 이 논문에서와 같이 선택적으로 방사화 핵종을 제거할 수가 없다. 전해제염에 대한 지속적인 기술개발을 통해 폐기물양을 줄이고 방사성 고가금속을 제한적으로 재활용 하는 것은 처분비용을 줄이고, 처분장을 효율적으로 이용하기 위한 것뿐 아니라, 국민들의 원자력산업의 사회적 수용성을 높이기 위해서도 반드시 필요하다.

주요어 : 지르코늄, 나이오븀, 압력관, 전해정련, LiCl-KCl, 순환전압법.

학 번 : 2014-21418